Antioxidant, Antimicrobial, Antidiabetic, Antiglycation, and Biocompatibility Potential of Aqueous *Zingiber officinale* Rhizome (AZOME) Extract

Mohd Hasan Mujahid [1], Tarun Kumar Upadhyay [1*], Vijay Jagdish Upadhye [2*], Prasanna Sriram Mathad [3]

Abstract

Background: The rhizome of *Zingiber officinale* or ginger shows its potential against oxidative stress, microbial infections, and managing diabetes mellitus. Method: Chemical reagents and plant materials of analytical grade were procured. Aqueous extract of *Zingiber officinale* rhizome was prepared through maceration. FT-IR, heavy metal detection, UV-VIS spectroscopy, and carbohydrate estimation were performed. Antimicrobial activity against bacterial and fungal strains was evaluated using agar diffusion method. Total polyphenol, flavonoid, and flavonol contents were quantified. Antioxidant activity was assessed using DPPH, reducing power, and FRAP assays. Antidiabetic activity was determined by α-amylase and α-glucosidase inhibition. Cytotoxicity, glucose uptake, and antiglycation assays were conducted on L6 cells. Blood compatibility was tested on human RBCs. Results: The analysis showed total phenolic content (TPC) at 27.9±0.27 mg/g GAE, total flavonoid content (TFC) at 18.4 mg/g QE, and total flavonol content (TFolC) at 41.1±4 mg/g QE. The extract demonstrated potent antioxidant activity with IC_{50} values of 353 µg/mL (DPPH), 600 µg/mL (H2O2 scavenging), and displayed antidiabetic effects inhibiting α-amylase (IC_{50}=1564.43 µg/mL) and α-glucosidase (IC_{50}=581.4 µg/mL). Cytotoxicity assays with an IC_{50} of 533.3 µg/mL (NRU assay) and highest glucose uptake at 254.74±62.79 µg/mL (L6 cells). The extract showed minimal hemolytic activity (-0.305±0.031%) and high cell viability, (99%) on Raw 264.7 a healthy cell line. *In silico* docking revealed strong interactions between AZOME's phytocompounds with targeted proteins (1b2y, 3top, & 7wsm). Conclusion: In conclusion, the aqueous extract of *Zingiber officinale* rhizome exhibits diverse pharmacological activities including antioxidant, antimicrobial, antidiabetic, and antiglycation properties, along with notable bio-safety and cytotoxicity profiles.

Keywords: Zingiber officinale rhizome, Antioxidant, Antimicrobial, Antidiabetic, Antiglycation, Biocompatibility, In silico

Significance | This study determined the therapeutic potential of Aqueous *Zingiber officinale* rhizome extract (AZOME) in combating oxidative stress, microbial infections, diabetes, and glycation-related complications.

*Correspondence. Tarun Kumar Upadhyay and Vijay Jagdish Upadhye. E-mail: tarun_bioinfo@yahoo.co.in, dr.vijaysemilo@gmail.com

Editor Fouad Saleh Resq Al-Suede, And accepted by the Editorial Board May 17, 2024 (received for review Mar 26, 2024)

Introduction

Plants have been integral to traditional medicine since ancient times. *Zingiber officinale* rhizome (ZOME) has been extensively utilized for its biological activities (Ali and Gilani, 2007), with a history spanning over 1500 years in systems such as Unani, Ayurveda, Siddha, and Chinese medicine (Upadhyay et al., 2024).

Author Affiliation.
[1] Department of Biotechnology, Parul Institute of Applied Sciences and Animal Cell Culture and Immunobiochemistry Lab, Research and Development Cell, Parul University, Vadodara, Gujarat, 391760, India.
[2] Department of Microbiology, Parul Institute of Applied Sciences and Research and Development Cell, Parul University, Vadodara, Gujarat, 391760, India.
[3] Department of Rasashastra and Bhaishajya Kalpana, Parul Institute of Ayurved and Research, Ishwarpura, Vadodara, Gujarat, 391760, India,

Please cite this article.
Mohd Hasan Mujahid, Tarun Kumar Upadhyay et al. (2024). Antioxidant, Antimicrobial, Antidiabetic, Antiglycation, and Biocompatibility Potential of Aqueous Zingiber officinale Rhizome (AZOME) Extract, Journal of Angiotherapy, 8(3), 1-20, 9660

ZOME harbors diverse phytoconstituents like shogaol, zingiberene, paradol, flavonoids, and gingerol, renowned for their antioxidant properties (Ali et al., 2008; Sivasothy et al., 2011; Nguyen et al. 2019). These bioactive compounds combat oxidative stress by neutralizing reactive oxygen species, thereby safeguarding cells and tissues from damage (Salehi et al., 2018; Huyut et al., 2017, Mostafa et al. 2024, Iza et al. 2024, Nur et al. 2023, Nurr et al. 2023, Javed et al. 2023, Hassan et al. 2018). Studies highlight ZOME's efficacy in reducing oxidative stress and countering infectious diseases, attributed to its rich phytochemical composition, including monoterpenoids, alcohols, and phenolic compounds (Eid et al., 2017). This underscores its potential as an antimicrobial agent and alternative therapeutic option against synthetic drugs (Beristain-Bauza et al., 2019). ;

Diabetes mellitus (DM) is a complex disorder affecting carbohydrate metabolism, leading to elevated glucose levels and subsequent damage to vital organs (Banday et al., 2020; Husen, 2023). Plant-derived phytoconstituents offer promising relief from diabetes-related complications, with phytomedicines presenting advantages over conventional drugs (Mohammadinejad et al., 2019). Key enzymes involved in carbohydrate breakdown, α-amylase, and α-glucosidase, were targeted to mitigate postprandial glucose spikes (Papoutsis et al., 2021). Diabetes also consists of the formation of advanced glycation end products (AGEs), exacerbating complications (Rhee and Kim, 2018; Nabi et al., 2019). *Zingiber officinale* rhizome (ZOME) is a recognized medicinal herb, although excessive use may lead to gastrointestinal discomfort (Yousfi et al., 2021).

The *in silico* method is increasingly employed in drug design, facilitating targeted therapy development cost-effectively and timelessly. Phytochemicals from medicinal plants targeting key anti-diabetic proteins like α-amylase and α-glucosidase, offer potential in lowering blood sugar levels (Jiang et al., 2020). This study explores the therapeutic potential of Aqueous *Zingiber officinale* rhizome (AZOME) extract in mitigating oxidative stress-related ailments, acting as an antioxidant and antimicrobial agent. Additionally, it addresses its role in managing diabetes mellitus and combating secondary complications through antiglycation properties. Computational analysis aids in identifying AZOME's impact on antidiabetic proteins (Jiang et al., 2020).

Materials and Methods

Chemical reagents and solvents

All the reagents and chemicals were of analytical grade. Mayer's reagent (Himedia), Sulphuric acid (Himedia), Lead (II) acetate trihydrate (Himedia), Ninhydrin solution (Himedia), Fehling A and B solution (Himedia). Standard drugs Gentamycin (Himedia), Ampicillin (Himedia), Chloramphenicol (Himedia), Ciprofloxacin (Himedia), Norfloxacin (Himedia), Nystatin (Himedia), Griseofulvin (Himedia), Muller Hinton agar media (Himedia), DMSO (Himedia), Potato dextrose agar media (Himedia), anthrone reagent (Himedia), Neutral red (3-amino-7-dimethylamino-2-methyl-phenazine hydrochloride) (Himedia), Glacial acetic acid (Merck), Ascorbic acid (Himedia), DPPH (Himedia), ABTS (2,2-Azino-bis (3-ethylbenzothiazoline-6-sulfonic acid) (Himedia), Quercetin (Himedia), Gallic acid (Himedia), Ferric chloride (Himedia), Aluminum chloride (Merck), Trichloroacetic acid (Himedia), Congo red (Himedia), Folin & Ciocalteu's phenol reagent (Himedia), Aminoguanidine hydrochloride (Sigma Aldrich) alpha-amylase (Himedia), alpha-glucosidase (Himedia), Sodium carbonate (Himedia), 2-Deoxy-D-glucose (Sigma-Aldrich, USA), Metformin hydrochloride (Sigma Aldrich)), Starch (Sigma-Aldrich, USA). All the chemicals and reagents used in the experimental work were of analytical grade.

Plant material

The *Zingiber officinale* rhizome (ginger) was procured from the local market Wagodia near Parul University, Vadodara, Gujarat, India. The recognition and validation of the Ginger rhizome was done by the Raw Drug Authentication Committee of Parul Institute of Ayurveda, Parul University. The certificate number: **PU/PIA/DG-Certi-222-1** was allotted for the submitted specimen and matched with the preserved specimen reference number: **PASM/PIA/DG/B-O/31**.

Preparation of Aqueous *Zingiber officinale* rhizome (AZOME) extract

The AZOME extract was prepared using a maceration process as previously done (Hafeez et al. 2023). In brief, *Zingiber officinale* rhizome was dried and powdered. 2 grams of dried powder was macerated overnight on a rotatory shaker using distilled water as a solvent in a 1:20 ratio. Afterward filtered with Whatman filter paper No.1, the solvent evaporated in the hot air oven as shown in (Figure 1), and then the extract was stored at -20°C for further use.

Chemical Characterization

FT-IR Analysis

The existence of organic and inorganic components in a sample can be determined using Fourier Transform Infrared Spectroscopy (FT-IR). The specific chemical groups present in the sample can be determined using spectrum data in automated spectroscopic software . The AZOME extract's FT-IR analysis was done on the Bruker ALPHA II compact FT-IR spectrometer using 22 scans from 3500 to 500 cm^{-1} using the OPUS software (Sahoo and Umashankara 2023).

Heavy metal detection

Heavy metal analysis was determined according to the mentioned protocol by (Kusse Gudishe Goroya et al. 2019) using a flame atomic absorption spectrophotometer (FAAS). In brief, the sample was prepared using the wet acid digestion method and further

analyzed through an Atomic Absorption Spectrophotometer; Model- AA 7000F (Japan).

UV-VIS Spectroscopy

The UV-VIS spectroscopy analysis was performed for the presence of characteristic absorption peak of phytochemical "Gingerol" in the *Zinger officinale* rhizome (ZOME) extract using a multi-mode microplate reader (synergy H1, BioTek, USA) as per the previously described protocol with slight modification (Saraf 2012). In brief, the sample was prepared at 1 mg/mL in distilled water, and a triplicate (n=3) manner spectrophotometrically spectrum was taken at a wavelength of 200-800 nm.

Carbohydrates estimation: Anthrone test

The Anthrone test is a simple method for the quantitative estimation of carbohydrates in different classes of samples like plant extracts, milk, blood serum, etc. The test was performed according to the mentioned protocol (Richards et al. 2020) with slight modifications. In brief, glucose stock solution (1 mg/ml) was prepared, and further diluted tenfold, glucose concentrations (200-1000 µg/mL) including an unknown sample (AZOME) extract. Freshly, prepared (0.2%) anthrone reagent in Sulphuric acid of which 3 mL was added to each test tube. Tubes were kept at a temperature of 90°C for 10 min in a water bath. Meanwhile, the carbohydrate gets reacted with concentrated Sulphuric acid to form furfural. Then furfural reacts with the anthrone reagent to give different shades of bluish-green complex solutions. The absorbance was taken at 630 nm of all samples spectrophotometrically on a multi-mode microplate reader (synergy H1, BioTek, USA).

Antimicrobial Assay

The antimicrobial susceptibility of ZOME aqueous extract was done against the selected microbial pathogen strains such as (MTCC 443) *Escherichia coli* (G^-), (MTCC 1688) *Pseudomonas aeruginosa* (G^-), (MTCC 96) *Staphylococcus aureus* (G^+), (MTCC 442) *Streptococcus pyogenes* (G^+) and fungus- (MTCC 227) *Candida albicans* (G^+), (MTCC 282) *Aspergillus niger* (G^+), *Aspergillus clavatus* (G^+).

Antimicrobial standard drugs

Gentamycin, Ampicillin, Chloramphenicol, Ciprofloxacin, and Norfloxacin for antibacterial activity, and Nystatin and griseofulvin for antifungal activity.

Antibacterial and antifungal susceptibility

The antibacterial and antifungal investigations of AZOME extract were determined previously mentioned protocol (Nariya et al. 2011). The agar diffusion method was applied for the antibacterial and antifungal activity of the AZOME extract. Sterile Muller Hinton agar media (Himedia) was created in Petri dishes. Separately, the bacteria (1x 10^8 bacteria/ml) were inoculated. in the media. Four wells in each petri dish (diameter 6 mm) were prepared in an aseptic environment. Aqueous ZOME extracts (5 µg/ml to 500 µg/ml) in various concentrations dissolved in DMSO. The same protocol was applied in the case of a standard drug. All of the dishes were incubated at the same time for 24 h at 37°C.

For the evaluation of antifungal susceptibility, in a petri dish potato dextrose agar media wasprepared . Afterward, fungus spores (1x 10^6 spores/ml) were inoculated in media and four wells with a 6 mm diameter were made under a sterile environment. The various concentration of ginger extracts (5 µg/ml to 500 µg/ml) was poured into these wells with DMSO as a blank. Afterward, all the Petri dishes were incubated at 37° C for seven days under aseptic conditions. The media was observed for the zone of inhibition by the various concentrations of extracts in respective wells. The zone of inhibition was measured with Vernier Caliper's help in a millimeter (mm) unit.

Preliminary Phytochemical Screening: Qualitative

The qualitative screening of phytochemicals such as alkaloids, steroids, flavonoids, terpenoids, saponins, phenol, amino acids, and reducing sugar was carried out using the previously mentioned protocol (Gohel et al. 2021).

Phytochemical Screening: Quantitative

Estimation of Total Polyphenol Content (TPC)

Total polyphenolic content was determined using the protocol mentioned (Fernandes et al. 2016). 1 mg/ml AZOME extract solution (100 µL) was mixed with 500 µL of 10% v/v Folin-Ciocalteau reagent (FCR), then mixed thoroughly on vortex and incubated for 2 minutes at room temperature. Afterward, 400 µL of 7.5% sodium carbonate was added and incubated for 15 minutes at 50° C. Then cooling to room temperature, a blue color was developed and absorbance was taken at 760 nm spectrophotometrically on a multi-mode microplate reader (synergy H1, BioTek, USA). Quantification of the total phenolic content was done by using a gallic acid (Hi-Media, Mumbai, India) standard curve taking in varying concentrations (50-250 µg/mL), and the result was expressed as gallic acid equivalents (GAE), milligrams per gram of dry weight (dw) as per the following formula: TPC (mg/g GAE) = C* V/M

Were, TPC is the mg/g of extract in gallic acid equivalent (GAE), "C" is the concentration of gallic acid from the calibration curve, "V" is the volume of extract in mL, while "M" is the dry weight (gm) of the raw material from which the extract was obtained.

Total Flavonoid Content (TFC)

The extract's flavonoid content presence was determined through the method adopted by (Oyedemi et al. 2012) with slight modification. Briefly, 1 mL solution of 2% w/v $AlCl_3$ in 100% methanol was added to the 1 mL of the sample solution and incubated for 1 hour at room temperature. After incubation appearance of a yellow color, formation took place, and absorbance was taken at wavelength 510 nm spectrophotometrically on a multi-mode microplate reader (synergy H1, BioTek, USA). Quantification of the total flavonoid content was done by using quercetin (purity

≥98%, Sigma–Aldrich, St. Louis, MO, USA) standard curve taken in varying concentrations (50-400 µg/mL) and the result was expressed as mg/g of quercetin equivalent (QE) as per the following formula: TFC (mg/g QE) = C* V/M

Were, TFC is the mg/g of extract in quercetin (QE); "C" is the concentration of quercetin from the calibration curve; "V" is the volume of extract, mL; while "M" is the dry weight (gm) of the raw material from which the extract was obtained.

Total Flavonols content (TFolC)

Quercetin was used as a reference standard for the evaluation of total flavonols content in the AZOME extract with sight modification as previously described method (Al-Mustafa et al. 2021). In brief 0.5 mL of sample/standard with different dilutions mixed with 1.5 mL of sodium acetate (50 mg/mL) and 0.5 mL of $AlCl_3$ (20 mg/mL) were combined. The reaction mixture absorbance was measured at 440 nm after the 2.5 h incubation and the reading was taken spectrophotometrically on a multi-mode microplate reader (synergy H1, BioTek, USA). Determinations were made in triplicate and the result was computed using the calibration curve produced from the quercetin.

Antioxidant Activity

Determination of total antioxidant activity: DPPH Assay

Any compound's anti-oxidant capacity can be assessed based on how well it scavenges the stable 2,2-diphenyl-1-picrylhydrazyl (DPPH) free radical. The assay was performed according to the mentioned protocol (Alsahli et al. 2021) with slight modifications. In brief, the stock solution of extract was prepared in distilled water and a series of different concentrations (50-500 µg/mL) were taken. In which a 3 ml solution of DPPH (0.1 mM) in methanol was mixed with various dilutions of AZOME extract. Standard ascorbic acid was used as a positive control, DPPH-methanol solution without extract as a negative control, and only methanol was used as a blank. The mixture was kept in the dark for 30 minutes at room temperature and absorbance was taken at 517 nm on a UV-visible spectrophotometer (UV-1900i, Shimadzu, Japan). The free radical scavenging activity (FRSA) percentage was calculated with the mentioned equation.

$$\% \text{ FRSA} = \frac{\text{Abs. of Control} - \text{Abs. of Sample}}{\text{Abs. of Control}} \times 100$$

Determination of Antioxidant capacity: Reducing Power Assay (RPA)

The ferric ion (Fe^{+3}) to ferrous ion (Fe^{+2}) reducing the power of the AZOME extract was performed according to the method described by (Oyedemi et al. 2017) with slight modification. In brief, different aliquots (50-500 µg/mL) were made from the stock solution of AZOME extract prepared in distilled water. To it 2.5 mL of Phosphate buffer (0.2 M, pH=6.6), and 2.5 mL of 1% Potassium ferrocyanide [K_4 Fe $(CN)_6$], then the reaction mixture is thoroughly mixed and covered with aluminum foil, incubated at 50° C for 20 minutes on a water bath. Afterward, 2.5 mL of Trichloroacetic acid (TCA), 10% (w/v) was added to each tube and centrifuge (Thermo Scientific Sorvall ST8R, USA) the solution at 3000 rpm, 5-6 minutes at 4° C. After centrifugation take the upper layer (2.5 mL) and add 2.5 mL of distilled water and mix properly. To this 0.5 mL (500 µL) of $FeCl_3$ (0.1 % w/v) was also added a bluish-colored solution was formed and absorbance was taken at 700 nm wavelength on a UV-visible spectrophotometer (UV-1900i, Shimadzu, Japan) and subsequently, ascorbic acid was used as a positive control and distilled water as a blank.

Determination of Ferric Reducing Antioxidant Power (FRAP)

The FRAP assay was performed according to the previously described method (Khan et al. 2022) to reduce the potential of aqueous ZOME by ferric ions with minor modifications. Different concentrations of AZOME extract (50-500 µg/mL) along with standard ascorbic acid, 100 µL added with the 3 mL FRAP reagent i.e., composed of 300 mM sodium acetate buffer (pH= 3.6), 10 mM TPTZ (2,4,6- Tri(2-pyridyl)-s-triazine solution), and 20 mM $FeCl_3$ in the ratio of 10:1:1 respectively. The mixture was incubated at 37°C for 30 min and reading was taken at 593 nm on a multi-mode microplate reader (synergy H1, BioTek, USA). At the same time, the results were expressed as µM Fe (II)/mg dry ZOME.

Hydrogen Peroxide (H_2O_2) Scavenging Activity

The ability of the AZOME extract to reduce the H_2O_2 and have antioxidant potential was investigated according to the lightly modified method of (Twereen et al. 2021). In short, the extract was taken in different concentrations (50-600 µg/mL) and suspended in phosphate buffer. A 43 mM hydrogen peroxide solution was prepared in phosphate buffer (0.1 M, pH 7.4). Different aliquots of extract were taken in the umber color falcon tube due to light sensitivity; the reaction should be performed in dark conditions. Then 3.4 mL of phosphate buffer (0.1 M) was added to each tube and 0.6 mL (600 µL) of 43 mM of hydrogen peroxide solution was also added, and the whole mixture was thoroughly mixed using a Digital vortex mixer (Thermo Scientific, USA). The absorbance of the solution was taken on a UV-visible spectrophotometer (UV-1900i, Shimadzu, Japan) at wavelength 230 nm after the incubation of 10-15 minutes at room temperature. A standard ascorbic acid was taken, phosphate buffer as a blank, and hydrogen peroxide solution (without extract) as a control was taken. The percentage of hydrogen peroxide scavenging activity was calculated using the following equation.

$$\% \text{ Scavenged } [H_2O_2] = \frac{\text{Abs. of Control} - \text{Abs. of Sample}}{\text{Abs. of Control}} \times 100$$

ABTS Assay

The antioxidant activity of AZOME extract was also found by using the 2,2'-azino-bis (3-ethylbenzothiazoline-6-sulfonic acid) (ABTS) radical scavenging activity as previously done by (Jung et al. 2022) with slight modification. In brief, the $ABTS^+$ radical solution was

prepared by mixing 2.4 mM potassium persulphate and 7 mM ABTS solution in equal volumes and keeping them in the dark at room temperature (25°C) to react with each other for 24 h. Afterward, the $ABTS^+$ solution was diluted with distilled water to get absorbance in the range of 0.7±0.01 units at wavelength 650 nm. AZOME extract (20 µL each) at different dilutions (50-500 µg/mL) was reacted with $ABTS^+$ solution (80 µL) in a 96-well plate and incubated for 4 min at room temperature. Then, the absorbance (λ=650 nm) was measured using a multi-mode microplate reader (synergy H1, BioTek, USA). A standard ascorbic acid was taken, distilled water as a blank, and $ABTS^+$ solution was taken as control. ABTS radical scavenging assay was calculated using the following formula.

ABTS radical scavenging assay (%) = [1- ($Abs._{Sample}$ – $Abs._{Blank}$) / $Abs._{Control}$] x 100

Antidiabetic Activity

***α*-Amylase Inhibitory Activity**

Alpha-amylase is an enzyme responsible for the breakdown of complex carbohydrates into simpler sugar moieties such as glucose. Inhibition of this enzyme can be beneficial for combating diseases such as metabolic disorders, obesity, and diabetes. We adopted the most acceptable procedure (Visvanathan et al. 2016), with a few minor modifications, to evaluate the AZOME extract performance in the *α*-Amylase inhibition experiment. In brief, we used a 96-well microplate in which enzyme solution 10 µL (20 mg/mL) was poured into each desired well. Samples dilutions (0-1000 µg/mL) were incubated for 10 min. Then 50 µL of the substrate (0.1 %) soluble starch was dissolved in PBS, the mixture was kept incubated for 15 min. Afterward, finally, 100 µL GOD-POD (glucose oxidase-peroxidase) reagent was added to the mixture and then incubated for another 10 min incubation at 37°C. Then, following the incubation absorbance was taken at 490 nm using a microplate reader (iMark; Bio-Rad, Germany). The inhibitor metformin was utilized as a positive control at a maximum concentration of 500 µg/ml.

Inhibition (%) =[(Ac-As)/Ac] x 100

Where, Ac = Absorbance of the control; As =Absorbance of the sample

***α*-Glucosidase Inhibitory Activity**

The *α*-Glucosidase enzyme plays a vital role in the small intestine by breaking down the disaccharides (such as maltose and sucrose) or complex carbohydrates into simple sugars (glucose) moiety (Warren et al. 2015). Inhibiting the action mechanism of *α*-Glucosidase can be beneficial for the diabetic person to manage the blood glucose level. The AZOME extract was tested for the inhibitory activity towards *α*-Glucosidase enzyme as previously mentioned protocol by (Telagari and Hullatti 2015) with slight modifications. In concise, the reaction mixture of 50 µL of phosphate buffer (100 mM, pH=6.8), 10 µL of *α*-Glucosidase (1 U/mL) enzyme, and 20 µL of AZOME extract concentration (0-1000 µg/mL). Afterward, in the reaction mixture 20 µL of P-NPG (4-Nitrophenyl-β-D- glucopyranoside) substrate was added and incubated for 20 min at 37 °C. The reaction was halted using 50 µL sodium carbonate (Na_2CO_3) [0.1 M]. Spectrophotometrically using an ELISA Microplate (iMark Bio-Rad, Germany) reader at the wavelength (λ=405 nm), the release of p-nitrophenol was assessed. As a positive control, Acarbose (1 mg/mL) was utilized. The results will be computed using the described formula and presented as % inhibition.

Inhibitory activity (%) = (1 − As/Ac) ×100

Where (As) is the absorbance in the presence of the test substance and (Ac) is the absorbance of control.

Cell culture maintenance

The rat myoblast (L6) skeletal muscle cells were purchased from the cell Repository, NCCS, Pune, India, and were cultured in the standard DMEM (Dulbecco's Modified Eagle's Medium). In Steri-Cycle® CO_2 Incubators from Thermo Scientific, cells were incubated at 37°C with 5% CO_2 and 10% FBS Gibco™ (Thermo Fisher Scientific), and 1% Antibiotic-Antimycotic solution was supplemented with the medium.

Cytotoxicity: NRU Assay

Cytotoxicity of the AZOME towards the L6 (myoblast) cell line was determined through neutral red uptake (NRU) assay as per the described method (Vajrabhaya and Korsuwannawong 2016) with slight modification. Cells were seeded in a 96-well plate with (5000-8000) cell/well density for 24 h supplemented with DMEM medium (10% FBS and 1% antibiotic solution). The next day, old media was removed and a fresh medium was added to each plate. Different concentrations of AZOME extract (1-1000 µg/mL) of 5µL were added in a triplicate manner including control without any extract treatment. The plate was incubated for 24 h in a CO_2 incubator at 37°C with a 5% CO_2 supply. Afterward, NRU (40 µg/ml in PBS) was added to the respective wells and incubated for 1 h. Following incubation, the medium was removed and added with 100 µL of NRU destain solution (EtOH/Glacial Acetic acid/Distilled water, 50%/1%/49%) to dissolve NRU. Then the absorbance was taken on an ELISA Microplate (iMark Bio-Rad, Germany) reader at a wavelength (λ=550/660 nm). Cell viability percentage calculated using the mentioned formula:

Cytotoxicity (%) = [(Control OD - Sample OD) / Control OD] x 100

***In vitro* Glucose Uptake Assay**

L6 cell lines were used as a model to investigate the glucose absorption by the muscle (skeletal) cells. The body's most prevalent tissue, skeletal muscle, is also the organ that uses postprandial glucose the most. The effect of the AZOME extract (133.32-533.3 µg/mL) on muscle glucose uptake in rat myoblast skeletal muscle (L6) cells was determined using the mentioned protocol

(Vishwanath et al. 2013) with slight modifications. L6 (rats' myoblasts) cells were seeded in 24 well plates with a density of 8 x 10^4 cells in each well incubated with standard DMEM (Dulbecco's Modified Eagle's Medium) medium for 24 h. After incubation cells were washed twice with KRPH (Krebs-Ringer-phosphate-HEPES) buffer (20 mM HEPES, 1 mM $CaCl_2$, 5 mM KH_2PO_4,136 mM NaCl, 4.7 mM KCl, pH=7.4), and then poured with glucose-free DMEM medium for 1 h. Afterward, cells were incubated for 40 min in KRPH buffer having 2% (v/v) BSA (Bovine Serum Albumin) and for 20 min in the presence and absence of 10 mM 2-DG (2-deoxyglucose). After washing the cells three times with PBS (Phosphate Buffer Saline) to remove the exogenous 2-DG, then sequentially lysed with the extraction buffer, frozen once and for 40 min heated at 85°C to degrade the endogenous NADP (Nicotinamide Adenine Dinucleotide Phosphate), and further centrifuged at 500 rpm for 2 min at 4°C.

After centrifugation the resulting supernatant was analyzed by GOD-POD (Glucose Oxidase-Peroxidase) Enzyme Assay Kit for 2-DG6P (2-deoxyglucose-6-phosphate) content and spectrophotometrically absorbance at λ = 505 nm was taken on a microplate reader (iMark Bio-Rad, Germany). For the blank, lysates of cells not exposed to 2-DG were taken, and calculation was based on nanomoles (nmol) of 2-DG by comparing the data with standard i.e., 2-DG6P (2-Deoxy-d-glucose). Insulin (0.1 U/mL) was used as a positive control (PC) and Metformin (1mM) was used as a negative control (NC).

Antiglycation Assays

D-Ribose-induced *in-vitro* glycation of BSA

To evaluate the inhibitory property of the AZOME extract towards the formation of formation of advanced glycation end products (AGEs) *in vitro* model was developed with slight modification as described by (Alvi et al. 2021). *In vitro* BSA glycation (antiglycation) assay was performed using model protein, BSA [0.5 mg/mL] (Bovine Serum Albumin), was incubated with the sugar [100 mM] (D-ribose, D-R), in the phosphate buffer saline [100 mM, pH=7.4, 37°C] (PBS), and with sodium azide [0.05%] (NaN_3) to avoid microbial growth in the mixture. The AZOME extract (2.5-100 µg/mL) and reference antiglycation agent Aminoguanidine (AG) hydrochloride (2.5-100 µg/mL) were taken and then the mixture with and without taking AZOME and AG incubated for the period of 7-days at 37°C. The BSA-DR (Glycated-BSA) was used as glycation control, only BSA (native) as control. Afterward the fluorescence spectra at Excitation: 360 nm and Emission: 440 nm were taken on a multi-mode microplate reader (synergy H1, BioTek, USA). The AG and AZOME were dissolved in doubled distilled water (ddH_2O).

Protein Aggregation Assay

In diabetic complications proteins from the usual fold form misfold leading to clump and enlarged structures called aggregates that interfere with normal cellular function. In brief human condition was simulated in *in vitro* condition using previously performed by (Nabi et al. 2018) with slight modification. In brief Glycated (Gly) means BSA (0.5 mg/mL) + D-R (D-ribose, 100 mM), BSA (0.5 mg/mL, unmodified), and AZOME extract (2.5-100 µg/mL) and Aminoguanidine or AG (2.5-100 µg/mL) treated with glycated BSA (Gly-BSA) samples were taken. The Congo red (CR, 100 µM, pH=7.4, 100 µL) was added to 500 of the above-mentioned samples and incubated for 20 min, and absorbance (λ=400 nm-700 nm) was taken to detect the amyloid detection in the Gly-BSA samples on a multi-mode microplate reader (synergy H1, BioTek, USA).

Hyperchromicity Investigation

When the biomolecules (nucleic acid, protein) attach with the sugar (glucose) moiety in a non-enzymatic reaction forming glycation products. There is an increase in the absorbance of light in these biomolecules due to a change in structure or conformation and the phenomenon is known as hyperchromicity (Nabi et al. 2020). We analyzed the effect of the BSA absorption pattern upon glycation and antiglycation, the UV-spectral analysis (200-800 nm) for the unmodified (BSA) and modified (Gly-BSA) as previously done with slight modification (Ashraf et al. 2015) for the period of 7 days. In brief, the native BSA (0.5 mg/mL) and glycated BSA (Gly-BSA): BSA (0.5 mg/mL) + D-ribose (100 mM) with and without the AZOME (2.5-100 µg/mL) extract/ Aminoguanidine (2.5-100 µg/mL) standard drug were taken. The reading was taken at 280 nm at a multi-mode microplate reader (synergy H1, BioTek, USA) and results were expressed as % hyperchromicity using the following equation.

% Hyperchromicity = [(Abs. of glycated sample-Abs. of native or Inhibitor-treated sample)/Abs. glycated sample] *100

To test the Biosafe nature of AZOME extract

Blood Compatibility Assay: AZOME against (Human) RBCs

Hemolysis assay or blood compatibility assay performed to evaluate the side effects of AZOME extract on blood. The blood compatibility of AZOME extract towards the human RBCs was performed with the procedure described by (Slowing et al. 2009) with minor modifications. In brief, blood was taken in a sterile condition from a healthy individual with proper consent. The blood in the EDTA vial was centrifuged (1500 rpm, 5 min, 4°C) to extract erythrocytes (RBCs) and serum was removed. Afterward, the RBC pellet was washed (3X), thrice with sterile NaCl (0.9%) solution, and at last same amount of NaCl solution was added. AZOME extract (40-120 µg/mL) concentration by our previous publication (Hasan Mujahid et al. 2023) for *in vitro* anticancer work was taken. Then RBC suspension (300 µL) was mixed with each AZOME extract. Positive Control (PC) and Negative Control (NC) were made by adding 300 µL of blood suspension to 1 mL of double distilled water (ddw) or Triton-X 100 (0.1%) and 0.9% NaCl solution respectively. After incubation (2 h) the samples were centrifuged (9000 rpm, 5

min, 4°C) to get a settled RBC pellet. The absorbance of the supernatant at λ=540 nm was measured using a multi-mode microplate reader (synergy H1, BioTek, USA) that is directly associated with the amount of hemoglobin released and % hemolysis can be calculated using the following equation.

% Hemolysis= [(Abs. of sample-Abs. of negative control)/ (Abs. of positive control-Abs. of negative control)] * 100

MTT Assay: Healthy cell line (Raw 264.7)

MTT assay is widely used to detect the cytotoxicity of the compound based on the colorimetric assessment of the cell viability and proliferation of cells. Generally, live cells contain NADPH-dependent oxidoreductase enzymes that convert MTT (3-[4,5-dimethylthiazol-2-yl]-2,5 diphenyl tetrazolium bromide) dye into formazan crystals. That is further used to assess the cellular metabolic activity of cells by assessing the production of purple color upon dissolved formazan crystals (Bahuguna et al. 2017). In brief, with slight modification $1x10^4$ cells/well (Raw 264.7) with complete media DMEM (100 µL) was seeded in a 96-well plate and incubated for 24 h at 37°C in the CO_2 incubator. Next day AZOME extract (25-1000 µg/mL) dissolved in incomplete DMEM media (100 µL) with complete media (100 µL) was treated Raw 264.7 cells. After incubation (24 h) media was removed and incomplete DMEM (100 µL) was added, then 10 µL of MTT dye (5 mg/mL in PBS) was also added and further incubated for 4 h. Formation of formazan crystals was visualized under Floid imaging system (EVOS® Floid cell imaging station, Invitrogen, Thermo Fisher Scientific, USA), and dissolved with 100 µL of DMSO (Dimethyl sulfoxide) per well after the old media was discarded. Then the plate was incubated for 15 minutes for complete dissolution of the formazan crystals. Afterward, the absorbance of the solution was taken at 490 nm with 570 nm as a reference wavelength on the multi-mode microplate reader (synergy H1, BioTek, USA). For the % viability calculation, the following formula was used:

$$\% \text{ Viability} = \left(\text{Abs. of} \frac{\text{sample}}{\text{control}} * 100\right)$$

***In Silico* Studies**

In continuation to explore the *in silico* antidiabetic effect of the Aqueous *Zingiber officinale* rhizome (AZOME) was performed by using the phytoconstituents (ligands) retrieved from our previous research work (Hasan Mujahid et al. 2023). Targeted protein moiety as enzyme inhibition role in diabetes such as 1B2Y (α-amylase), 3TOP (α-glucosidase), and glucose transporter protein 7wsm (GLUT4) was selected. The study was performed using multi-computational tools such as CB-Dock2 (Liu et al. 2022) online web server, AutoDock version 4.0 of PyRx software (Trott and Olson 2010), and AutoDock 4.2 Tools (Valdés-Tresanco et al. 2020) to check and compare docking score variability among different virtual docking tools. As usual, ligands 3D SDF format downloaded retrieved from PubChem (www.pubchem.com) database, and protein moiety was downloaded from Protein Data Bank (https://www.rcsb.org/), visualization tool BIOVIA Discovery Studio Visualizer, LigPlot+ v.2.2.8 program, and file format exchange tool Open Babel software was used.

Preparation of Ligand and Protein

CB-Dock2

CB-Dock2 is an online server platform for ligand and protein docking. Protein in PDB format and ligand in any of mol2, mol, SDF, or PDB was needed to perform the docking.

PyRx

Protein was downloaded from Protein Data Bank (PDB) and opened in the visualizing tool "BIOVIA Discovery Studio" to remove water molecules, Hetero atom (Hetatm), inhibitors, or ligands in the existing protein. A polar H-atom was added (Chemistry→Hydrogen→Polar) to the protein and saved in the PDB format. The in-built Open Babel GUI was used to convert the SDF format of phytochemicals (ligands) downloaded from the PubChem database.

AutoDock Tools

To begin with, the protein was prepared by removing all water molecules (Edit→Delete water). If the protein of interest has two or more chains, then the main chain should be kept and the rest must be deleted (Select→String→Chain list→Choose chain→Click on add→Dismiss→Go to edit→Click on delete→Click on delete selected atoms→Continue). Then, polar hydrogen (Edit→Hydrogen atoms→Add→Choose polar hydrogen) and Kollman charges (Edit→Choose charges→Kollman charges) were added. Finally, save the protein to PDBQT format through (Edit→Atoms→Assign AD4 type→Save option→Choose PDBQT), and the protein is prepared now. For the ligand preparation (Click ligand→Input→Open→Select PDB format of ligand→Open→Click OK). Next go to ligand (Torsion tree→Choose root), again go to ligand (Torsion tree→Detect Root). Click ligand (Output→Save as PDBQT with PDBQT extension→Save). Now both protein and ligands were finally prepared for further steps for docking.

Statistical Analysis

Data collection and summarization were initially carried out using a Microsoft Excel Worksheet and analysis of variance (ANOVA) was performed on GraphPad Prism 8.0 with a significant *p-value* at <0.05 and data was also analyzed with Origin Pro 2024 (Origin Lab Corporation, Hampton, MA, USA). Each reading was recorded three times, and the results were presented as means ± standard deviation (SD) or percentage.

Results

AZOME extract preparation

The aqueous *Zingiber officinale* rhizome (AZOME) extract was prepared using the cold-maceration process. The AZOME extract

produced was 0.1445 gm (144.5 mg), yielding 7.2 % from the 2-gm dry raw material.

Functional group analysis: FT-IR

The distinctive functional groups in the bioactive molecule (phytochemical) in the ZOME extract were identified using Fourier transform infrared (FT-IR). The sample was scanned from 3500 to 500 cm^{-1}. Qualitative phytochemical functional group analysis of unprocessed ZOME (raw) and processed AZOME extracts FT-IR wave number (cm^{-1}) were mentioned in (Supp. Table 1)In contrast, individual FT-IR spectra of ZOME, AZOME extract, and merged spectra can be depicted in (Figure 2 (A-C).

Heavy metal analysis

The levels of heavy metals such as Iron (Fe), Lead (Pb), Cadmium (Cd), Copper (Cu), Manganese (Mn), Nickel (Ni), and Zinc (Zn) were determined in the AZOME extract using FAAS. The concentration of various heavy metals in parts per million (ppm) in the AZOME extract in the following trend: Fe>Zn>Mn>Cu>Pb>Ni>Cd as mentioned in (Figure 3A).

UV-VIS Spectra

The characteristic peak of the phytoconstituent of AZOME extract "Gingerol" shows a maximum absorption peak at the wavelength of 280-282 nm with an absorption value of 3.842 represented in (Figure 3B).

Carbohydrate content: Anthrone test

The Anthrone test was done for the evaluation of carbohydrate content in the aqueous *Zingiber officinale* extract. The working solution (200-1000 µg/ml) was prepared from a diluted stock solution of D-glucose (1 mg/ml), and an unknown sample. The absorbance (λ=630 nm) was taken using the spectrometer technique and a graph was plotted showing the mean absorbance value and different glucose concentrations containing solution with the unknown sample. The amount of carbohydrate in the unknown sample in AZOME extract was extrapolated from the standard D-glucose curve was 247.96 µg/ml as shown in (Figure 3C). A significant *p-value* of 0.002854 ($P<0.05$) was found among all mean values of absorbance with the green or blue color indication in the samples.

Antimicrobial activity

The results demonstrated that the extract of AZOME has efficient antibacterial and antifungal activity against the examined standard strains. The extrapolation of the zone width (in mm) of concentration (5-500 µg/mL) inhibition and the MIC findings of AZOME extract with the available standard drug was observed (Supp. Table 2). No clear zone of inhibition was found at 5 µg/mL, while 500 µg/mL concentration showed a maximum zone of inhibition with 21 mm (Supp. Table 3). The lowest concentration (MIC) of AZOME extract and standard drugs as an antibacterial agent against the standard strains with AZOME was MIC of 100 µg/mL towards *E. coli* and *S. aureus* strains, and standard drug Gentamycin having 0.05, 1, 0.25, and 0.5 µg/mL towards *E. coli*, *P. aeruginosa*, *S. aureus*, and *S. pyogenes* respectively (Supp. Table 4). The antifungal activity of AZOME extract with MIC 100 and 125 µg/mL was observed towards *C. albicans* and *A. clavatus* respectively with standard antifungal drugs also.

Phytochemical Investigation

A phytochemical analysis confirmed the presence of components mentioned in (Supp. Table 5) such as saponins, terpenoids, reducing sugar, molish test (carbohydrate), phenols, alkaloids, and amino acids (Figure 4).

Total Phenolic Content

The AZOME extract's total phenolic content, measured as the gallic acid equivalent of phenols, was determined by the Folin-Ciocalteau technique. The amount of phenolic content found in AZOME extract was 27.9±0.27 mg/g GAE dw extrapolated from the calibration curve of gallic acid (50-250µg/ml) shown in (Figure 5A).

Total Flavonoid Content

Total Flavonoid Content (TFC) in the AZOME extracts was extrapolated using quercetin equivalent to the flavonoid, standard calibration curve. The concentration of quercetin standard curve showing the AZOME extract has 18.4 mg quercetin equivalent (QE)/g of TFC is depicted in (Figure 5B).

Total Flavonol Content

The amount of total flavonol content (TFolC) in the AZOME extract was extrapolated by using the standard calibration curve of Quercetin mentioned in (Figure 5C). The total flavonol content was found to be 41.4±4 mg/g QE.

DPPH Assay

Free radical scavenging activity of AZOME extract was performed using DPPH assay. It showed efficient percentage radical scavenging activity (RSA) and increased in a concentration-dependent manner as shown in (Figure 5D). AZOME extract adds an electron to the DPPH solution (purple color), free radical into a creamy (yellowish) solution. The inhibitory concentration (IC_{50}) to scavenge free radicles by AZOME extract was found to be 353 µg/mL and the standard (ascorbic acid) was 50 µg/mL.

Reducing power assay: Fe^{3+} reducing power

The findings of the evaluation of the AZOME extract capacity to convert Fe^{3+} to Fe^{2+} are shown in (Figure 5E). The results revealed that the reducing power of the AZOME extract significantly increased in a dosage-dependent manner (50-500 µg/mL).

FRAP Assay

FRAP (Ferric Reducing Antioxidant Power) experiment was carried out to establish the antioxidant capacity of AZOME extract further and expressed in terms of ferrous sulphate equivalent (mM/g of sample). (Figure 5F) shows that AZOME extract has an increasing dose-dependent ferric-reducing ($Fe^{+3} \rightarrow Fe^{+2}$) antioxidant activity. The measured absorbance was 0.217, 0.274, 0.403, 0.559,

0.693, and 0.866 at a varied concentration of 50, 100, 200, 300, 400, and 500 µg/mL respectively.

Hydrogen Peroxide Scavenging Capacity

The scavenging ability of AZOME extract on hydrogen peroxide (H_2O_2) is shown in (Figure 5G). The AZOME extract was capable of scavenging hydrogen peroxide-free radicals in an amount-dependent manner (50-500 µg/mL) and showed maximum scavenging activity and an IC_{50} value of 600 µg/mL.

Radical scavenging activity: ABTS Assay

The radical scavenging activity of AZOME extract was determined using the 2,2'-azino-bis (3-ethylbenzothiazoline-6-sulfonic acid). The percentage of radical scavenging activity was found to increase as the concentration of AZOME extract and standard increased. The relative capacity of antioxidants to scavenge the ABTS+ radicals of AZOME extract ranged from 53-63%. In comparison positive control ascorbic acid (50-500 µg/mL) ranging from 92-93% can be evaluated in (Figure 5H)

Carbohydrate-digesting enzymes: α-Amylase Inhibition

The results of α-amylase enzyme inhibitory activities through AZOME extract (31-1000 µg/mL) with the positive control (PC) standard drug "Metformin" (500 µg/mL) and final concentration were shown in (Figure 6A). The inhibitory action of AZOME extract was found to be 15-25 % and the IC_{50} value of 1564.43 µg/mL (1.5644 mg/mL) while metformin (PC) showed 70% inhibitory action towards the α-amylase enzyme.

Carbohydrate-digesting enzymes: α-Glucosidase Inhibition

The ability of the AZOME extracts (10-1000 µg/mL) with Acarbose (1 mg/mL) as a positive control drug was used to inhibit the α-Glucosidase enzyme activity *in vitro* conditions as shown in (Figure 6B). The inhibitory action of AZOME extract was found to be 10% at (10 µg/mL) and highest up to 51% (1000 µg/mL) in a dose-dependent way with an IC_{50} value of 581.4 µg/mL while acarbose (PC) showed 69% inhibitory action towards the α-Glucosidase enzyme.

Neutral red cytotoxicity test

The viability of the L6 (rat myoblast skeletal muscle) cell line was assessed at increasing concentrations (1-1000 µg/mL) of the AZOME extract using the NRU assay. The AZOME extract has significant cytotoxicity towards the L6 cell line in a dose-dependent manner as shown in (Figure 7A-B) with neutral red uptake by cells. The percentage cell viability of the L6 cell line with IC_{50} value 533.3 µg/mL is shown in (Figure 8A).

Glucose uptake assay

The glucose uptake activity of AZOME extract was measured on the L6 cell line at different concentrations (133.32-533.3 µg/mL) and the outcomes were compared with metformin (negative control) and insulin (positive control) drugs available for diabetes mellitus (DM) medications. AZOME extract has the highest glucose uptake activity with a mean glucose concentration of 254.74±62.79 µg/mL, 132.73±32.60 µg/mL, and 117.01±23.66 µg/mL at 533.3 µg/mL, 266.65 µg/mL, and 133.32 µg/mL respectively. In comparison, **Insulin** [0.1 U/mL] (244.51±30.37 µg/mL) as a positive control and **metformin** [1 mM] (49.90±6.96 µg/mL) as a negative control were used in the experimental setup as shown in (Figure 8B).

Effect of AZOME extract on BSA-AGE formation

The test samples AZOME extract (2.5-100 µg/mL) and standard antiglycation (2.5-100 µg/mL) agent (Aminoguanidine) showed a decrease in the fluorescence spectrum at the end of the seven-day incubation period as shown in (Figure 9A). (Figure 9B) shows the relative percentage of advanced glycation end products (AGEs). The glycation product, positive control, BSA conjugate D-Ribose (BSA+D-R) showed 100% AGEs formation. The test sample AZOME extract decreased the AGEs (%) from 63.50% ± 1.07 to 58.59 % and AG showed 67.12% ± 1.75 to 51.99 % ± 3.08 compared to a positive control (BSA+DR).

Protein aggregation via Congo red binding

The protein aggregation assay was performed to simulate the glycation (Gly) product formed in a diabetic patient due to an amalgamation of sugar molecules with the protein moiety using the Amyloid-specific Congo red (CR) binding assay. We found that enhanced CR-absorption (82.55%) in Gly-BSA (BSA+D-ribose) in comparison to native unmodified BSA (only BSA). However, we found a decrement in the absorption when treated with different concentrations of standard drug, (AG) aminoguanidine (2.5-100 µg/mL) and AZOME extract (2.5-100 µg/mL). AG reduced the CR-specific absorbance maximum from 79.57 % to reduce to 26.33 % shown in (Figure 10A). Moreover, AZOME extract also exhibits a significant reduction from 87.32 % to 51.26 %, as depicted in (Figure 10B).

Hyperchromicity assay

The increase in absorbance (hyperchromicity) found in the UV-Vis spectrum (200-800 nm) showed that 100 mM (D-ribose) caused 97.01% BSA glycation (BSA+D-ribose) on the 7th day as compared to native-BSA (2.2%). The addition of standard drug aminoguanidine (AG) at concentrations (2.5-100 µg/mL) to Gly-BSA samples marked a decrement in the % hyperchromicity ranging between 4.14 % at (2.5 µg/mL) to 2.09 % at (100 µg/mL) concentration as shown in (Figure 10C. A similar reduction in hyperchromicity was also found in the case of treatment of AZOME extract towards Gly-BSA samples that showed 7.5 % at (2.5 µg/mL) to 3.47 % at (100 µg/mL) concentration as mentioned in (Figure 10D).

Hemolysis assay

In vitro, the biocompatibility of the AZOME extract was performed to check the biosafe nature of the plant-based extract. For these fresh erythrocytes, red blood cells (RBCs) were exposed to the AZOME extract (40-120 µg/mL) concentrations, and the % hemolysis result revealed hemolysis up to -0.399±0.020, -

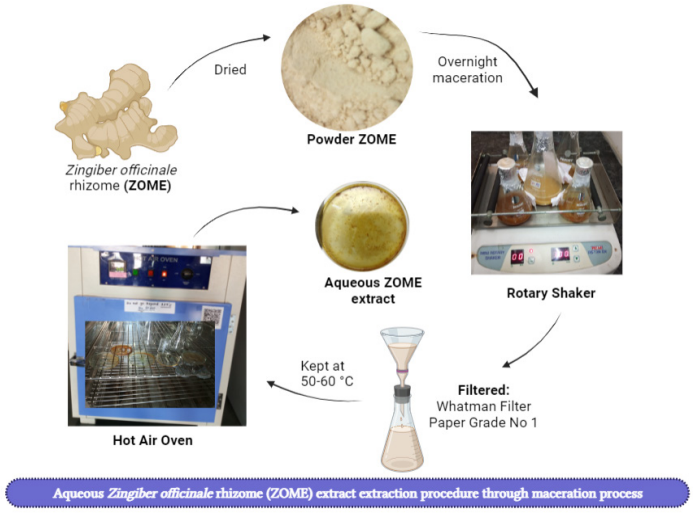

Figure 1: Aqueous extract of *Zingiber officinale* rhizome (ZOME) was prepwered using a maceration process.

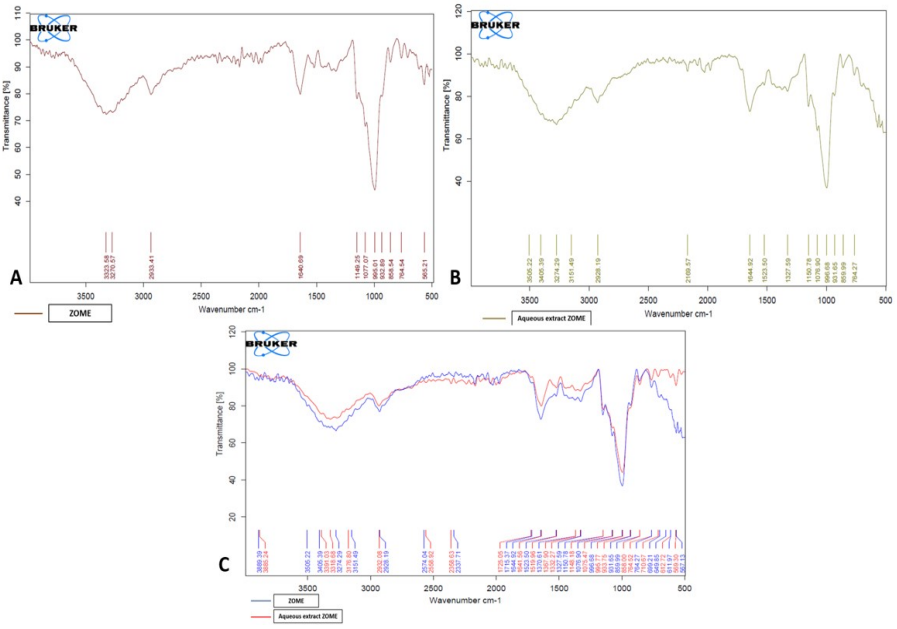

Figure 2: Representative FTIR spectrum of ZOME. (A); The spectrum of raw ZOME (B); Spectrum of AZOME extract (C); Overlay spectrum of raw ZOME and AZOME extract to observe the shifting (wavenumber) of the functional group.

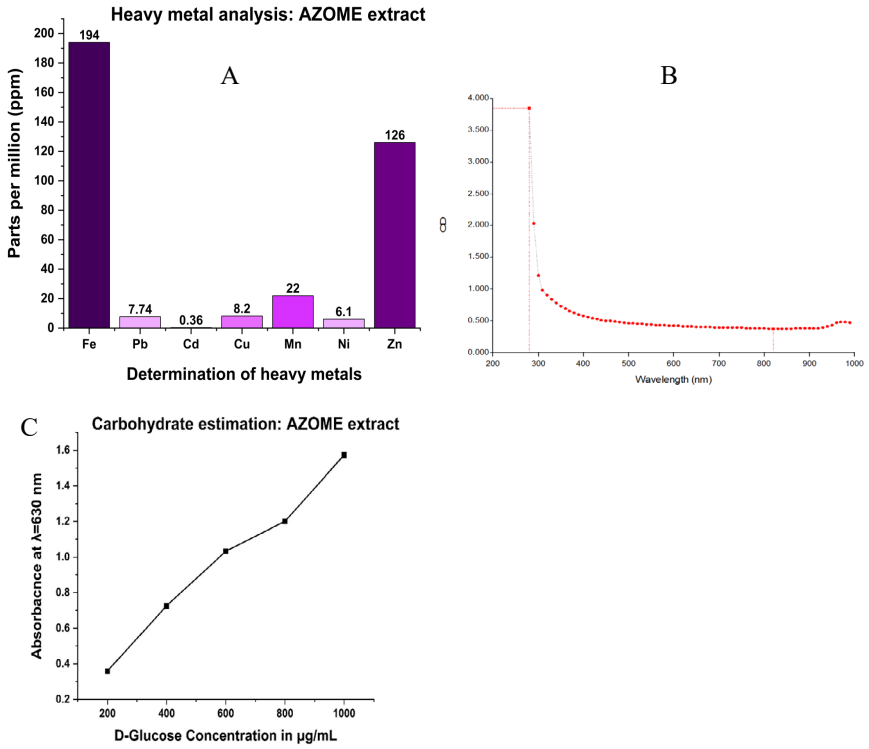

Figure 3: (A) Heavy metals detection in AZOME extract. The trace elements: Iron (Fe), Lead (Pb), Cadmium (Cd), Copper (Cu), Manganese (Mn), Nickel (Ni), and Zinc (Zn) amount in AZOME extract were mentioned in parts per million (ppm). (B) UV-VIS Spectra of AZOME extract for the identification of phytoconstituent Gingerol. (C) Carbohydrate estimation in AZOME extract using anthrone test.

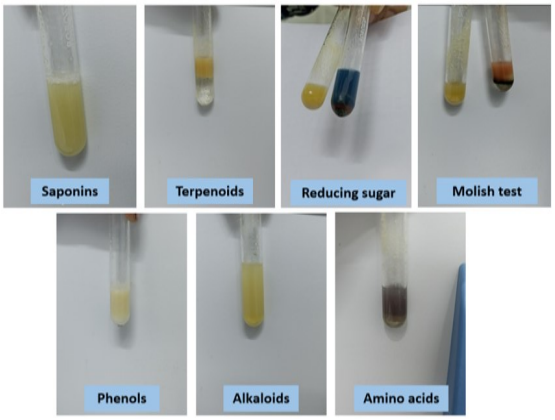

Figure 4. Pictorial representation of qualitative phytochemical screening of AZOME extract. Showed the presence of various secondary metabolites identified through color change.

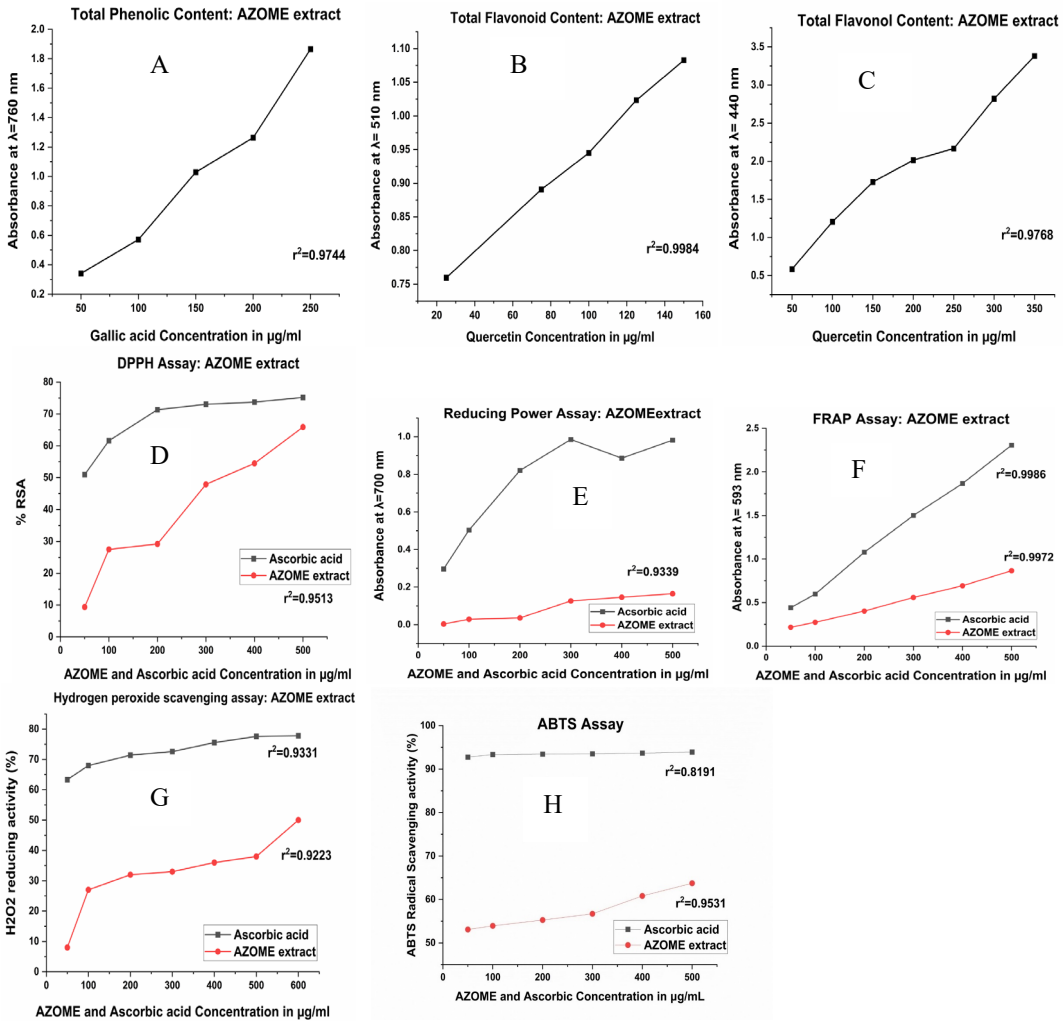

Figure 5. (A) TPC in AZOME extract using Standard gallic acid at various concentrations (50-250µg/ml). All the values were presented by mean ± SD. (B) Total Flavonoid Content in AZOME extract extrapolated using standard quercetin at various concentrations (25-150µg/mL). All the values were presented by mean ± SD. **(C)** Total Flavonol Content in AZOME extract extrapolated using standard quercetin at various concentrations (50-350µg/mL). All the values presented by mean ± SD were determined in a triplicate manner. (D) AZOME extract showed a significant increase in radical scavenging activity (RSA) and a maximum % RSA was reported at 500 µg/ml. Values were represented by mean ± SD. (E) AZOME extract showed an efficient increase in reducing power (Fe^{3+} to Fe^{2+}) in a concentration (50-500 µg/mL) dependent manner. Values were represented by mean ± SD. (F) Ferric reducing antioxidant power of AZOME extract. Showed a significant increase in the absorbance as the concentration of AZOME extract and standard drug increased. Values were represented by mean ± SD. (G) AZOME extract showed H_2O_2 lowering action as increased in a concentration-dependent way (50-500 µg/mL). Values were represented by mean ± SD. (H) ABTS, 2, 2'-azino-bis (3-ethylbenzthiazoline-6-sulphonic acid) scavenging activity. AZOME extract with ascorbic acid (standard drug) antioxidant property to scavenge $ABTS^{+}$ radical increases in a concentration-dependent manner. All values were represented by mean ± SD.

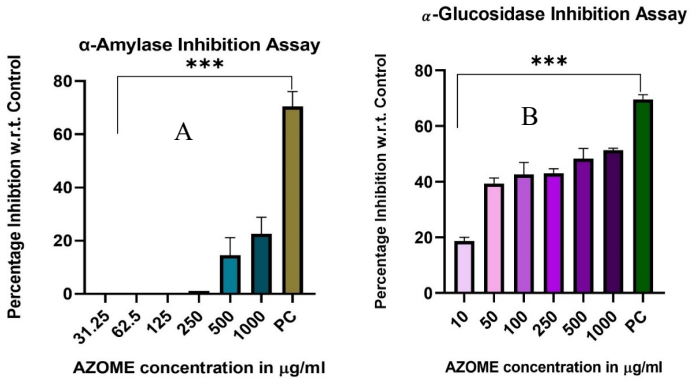

Figure 6. (A) α-amylase enzyme inhibitory activity of AZOME extract. Metformin was used as a standard or positive control. Mentioned values were mean ± SD (n=3). (B) α-glucosidase enzyme inhibitory activity of AZOME extract. Acarbose was used as a positive control (PC). The mentioned values were mean ± standard deviation.

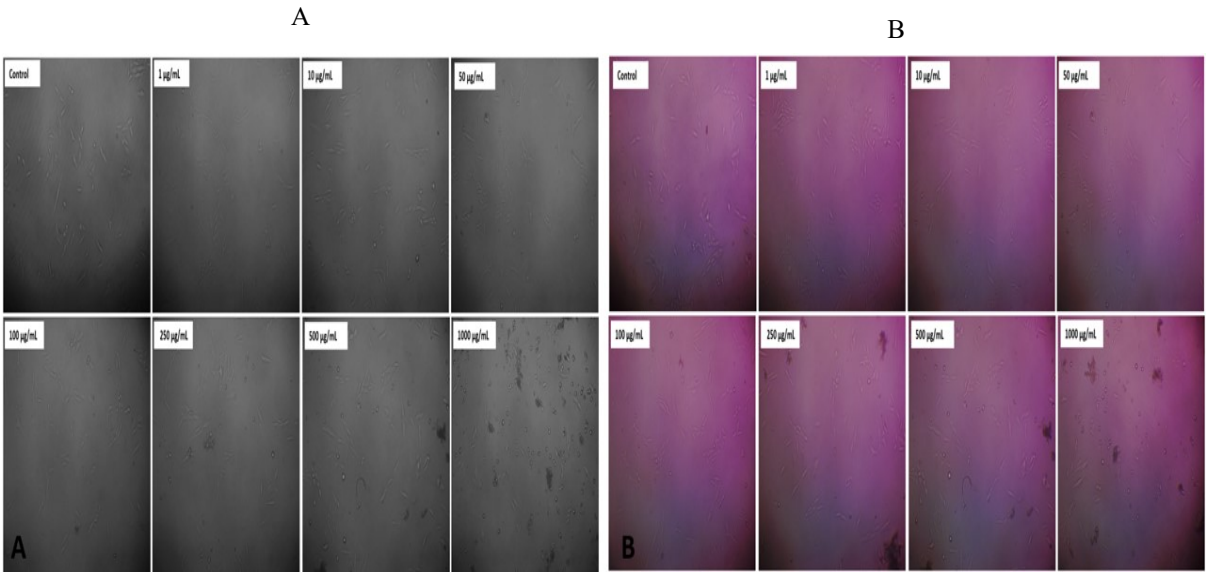

Figure 7 (A); Evaluation of the cytotoxic effect of AZOME extract on L6-cell line morphology after the treatment (24 h), (B); NRU assay was performed and visualized using an Olympus CK2 under a 10X magnification inverted microscope that illustrates the L6 cell's intracellularly bound neutral red dye.

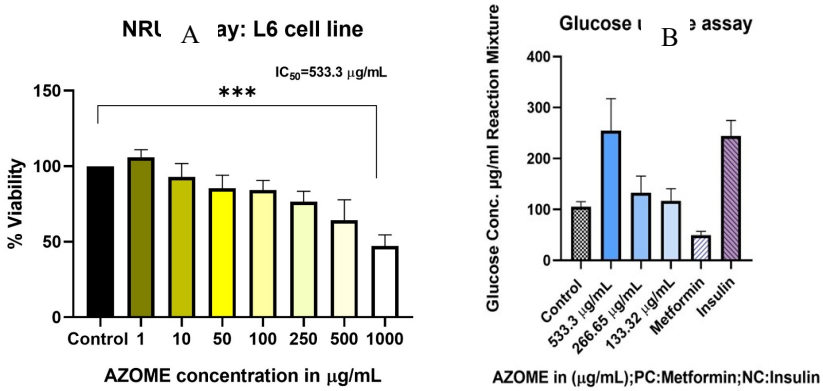

Figure 8. (A) Cell cytotoxicity was observed after 24 h of treatment with AZOME extract showing an IC_{50} value of 533.3 µg/mL against the L6 cell line. Represented values were mean ± SD with $^{***}p<0.001$ value. **(B)** Glucose uptake activity of the AZOME extract at different concentrations (133.32-533.3 µg/mL) on the L6 cell line compwered to the Insulin: Positive control (PC) and Metformin: Negative Control (NC) as available standard antidiabetic drugs.

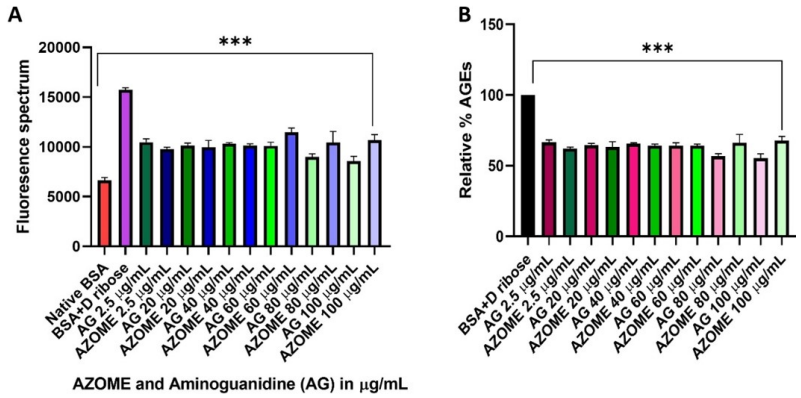

Figure 9. Estimation of antiglycation activity. (A); Fluorescence spectrum ($\lambda_{Ex.}$=360 nm and $\lambda_{Em.}$=440 nm) showing the lowest spectrum of native BSA, the highest fluorescence spectrum of BSA+D ribose (positive control), and a decrement (±) in the fluorescence spectrum found in standard antiglycation agent: aminoguanidine and the AZOME extract. (B); The decrease in the relative percentage of AGEs (% AGEs) was found due to the presence of AZOME extract treatment and aminoguanidine drug in a concentration-dependent manner (2.5-100 µg/mL). Results were expressed as mean ± SD with a significant $^{***}p<0.001$ value.

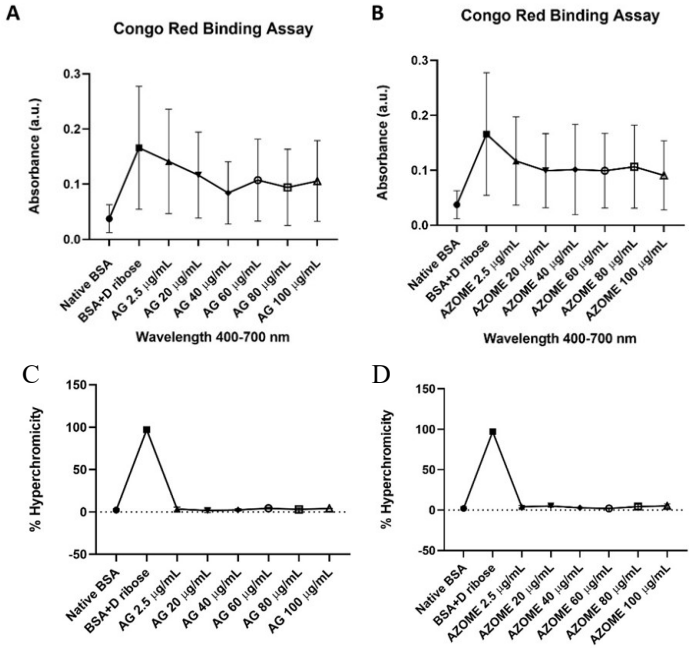

Figure 10. Protein aggregation detection using Congo red binding assay. (A); Native BSA, Gly-BSA (BSA+D-ribose), and Aminoguanidine (AG) treated Gly-BSA model, and absorbance was recorded in the 400-700 nm range. (B); Native BSA, Gly-BSA (BSA+D-ribose), and AZOME extract-treated Gly-BSA experimental setup. The data represented the Mean ± SD values. (C); The % hyperchromicity in Native or unmodified BSA, Gly-BSA (BSA+D-ribose), and the effect of Aminoguanidine (AG) (2.5-100 µg/mL) on the Gly-BSA model. (D); Showed % hyperchromicity in native-BSA, modified BSA (Gly-BSA), and treated effect of AZOME extract towards Gly-BSA. The data represented were the mean ± SD.

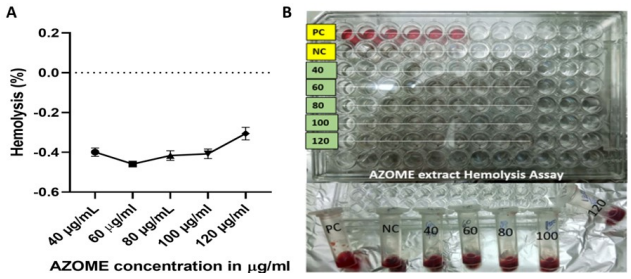

Figure 11. Biocompatibility analysis of AZOME extract using hemolysis assay. (A); Graphical representation of Hemolysis % of AZOME extract (40-120 µg/mL) showed RBCs reduction ranging. The data represented were the mean ± SD with significant ****p-value* (<0.0001). (B); Experimental setup visualization showing centrifuge tubes after centrifugation step and 96-well plate for taking reading where positive control (PC): tap/distilled water, negative control (NC): NaCl solution, and for biocompatibility test AZOME extract (40-120 µg/mL) was taken.

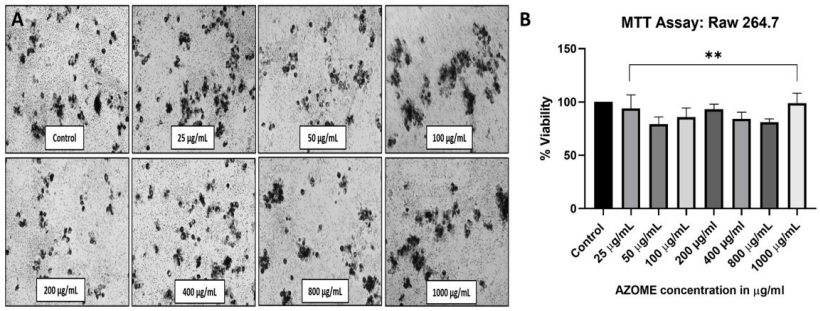

Figure 12. The proliferative nature of AZOME extract towards a healthy cell line, RAW 264.7. (A); Showed the formation of formazan crystals after incubation (4 h) with the treatment of MTT dye. (B); The column-graphical representation shows the % viability of the RAW 264.7 cells on exposure to AZOME extract (25-1000 µg/mL) showing the dose-dependent proliferative effect. The represented data is the mean ± SD values with significant ***p-value* (0.0018) <0.05.

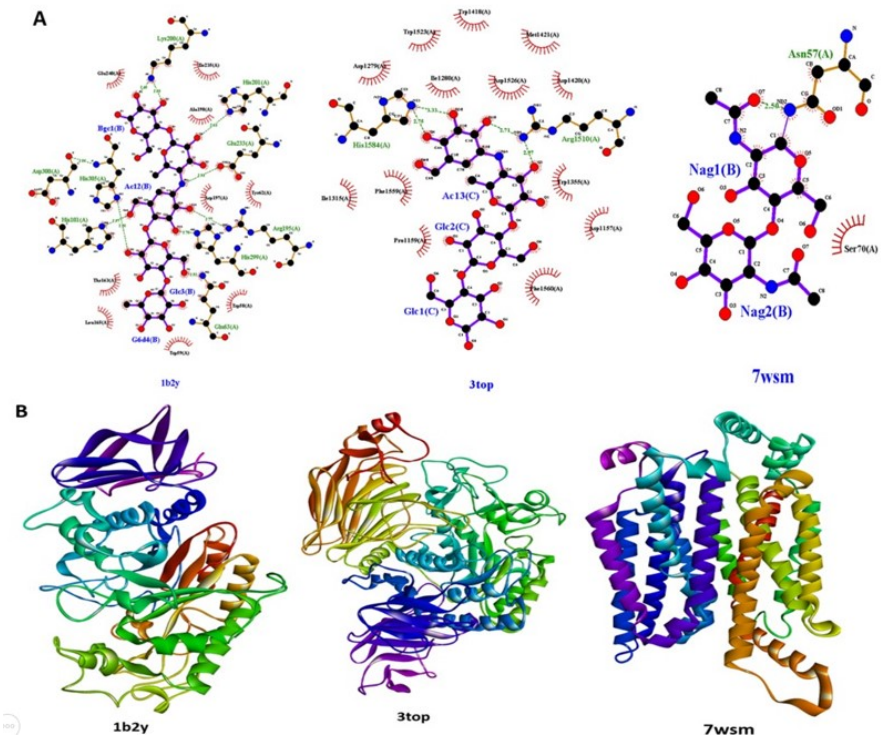

Figure 13. (A); **2D** representation of targeted antidiabetic proteins PDB ID: 1b2y (alpha-amylase); 3top (alpha-glucosidase) and 7wsm (GLUT4) visualized using 2D interaction map (LigPlot+ v.2.2.8) program and (B); **3D** visualization of prepwered proteins using BIOVIA Discovery Studio Visualizer.

0.458±0.012, -0.416±0.024, -0.407±0.024, and -0.305±0.031 % at a varying concentration of 40-120 µg/mL respectively can be visualized in (Figure 11A). Biocompatibility of AZOME extract can be seen as it doesn't induce erythrocyte lysis, resulting in no release of hemoglobin into the extracellular environment that can be seen after the centrifugation step to take a reading (λ=540 nm) in 96-well plate as shown in the (Figure 11B).

Cytotoxicity assessment

The RAW 264.7 cell line was used to assess the biosafety nature of the AZOME extract. There was no obvious cytotoxicity found in the Raw 264.7 cell line treated with AZOME extracts (25-1000 µg/mL) with a minimum of ~1% to a maximum of ~20% was observed. The visualization of formazan crystals can be depicted in (Figure 12A) The percentage (%) viability of the Raw 264.7 cell line treated with AZOME extract showed a proliferative nature with of minimum % viability of 79% to a maximum of 99% of the cells in a concentration-dependent manner as shown in (Figure 12B)

Molecular docking studies

The molecular docking was performed on the varied software viz., CB-Dock2, PyRx, and Auto Dock Tools to find out the variability in the binding affinity (kcal/mol) using the phytochemicals (ligands) obtained through GC-MS analysis of AZOME extract towards the targeted antidiabetic proteins such as Alpha-amylase (1B2Y), Alpha-glucosidase (3TOP), GLUT4 (7WSM) as shown in (Figure 13A-B). To validate the finding in the *in vitro* assay regarding enzyme inhibition assay and glucose uptake assay in the L6 cell line molecular docking was performed (Supp. Table 6). The complex for the targeted protein and ligands with interacting amino acids with atom residue (Supp. Table 7).

Discussion

The history of plant-based healing, known as phytomedicine, spans from ancient traditions dating back 60,000 years to written records 5,000 years ago (Kurhekar, 2021). *Zingiber officinale* rhizome, a household spice, is among these medicinal plants. The aqueous extract of *Zingiber officinale* rhizome (AZOME) was obtained through cold maceration with a yield of 7.2%. FT-IR analysis revealed various phytocompounds in AZOME, including phenolics, proteins, polysaccharides, terpenes, and alkaloids (Akbari et al., 2019).

The detection of heavy metals using a Flame Atomic Absorption Spectrophotometer (FAAS) was conducted, ensuring the quality, safety, and sustainability of drug development and scientific research. The presence of trace metals in the AZOME extract was quantified: Fe (194 ppm), Zn (126 ppm), Mn (22 ppm), Cu (8.2 ppm), Pb (7.74 ppm), Ni (6.1 ppm), and Cd (0.36 ppm). These trace elements, including essential ones like Iron (Fe), Zinc (Zn), Manganese (Mn), and Copper (Cu), and non-essential micronutrients such as Lead (Pb), Nickel (Ni), and Cadmium (Cd), play pivotal roles in biological systems. However, they can become hazardous if their concentrations exceed recommended levels (Shah et al., 2013). The UV-Vis spectrum of the AZOME extract exhibited a prominent peak between 280-282 nm, characteristic of "Gingerol," the major phytoconstituent of ZOME.

The gingerol compound exhibits potent antioxidant properties, combating oxidative stress and diabetes mellitus and demonstrating antimicrobial activity (Ma et al., 2021). It effectively scavenges free radicals, neutralizing harmful reactive oxygen species that can damage cellular organelles and increase the risk of chronic diseases such as heart diseases, diabetes, cancer, and neurodegenerative diseases.

Proximate analysis revealed that the AZOME extract contains 247.96 µg/mL of carbohydrates, determined using the anthrone method of detection. Studies propose ginger rhizomes typically comprise 60-70% carbohydrates (Srinivasan, 2017).

In our investigation, the AZOME extract displayed efficient antibacterial and antifungal activities. The minimum inhibitory concentrations (MIC) were determined to be 100, 125, 100, and 125 µg/mL for *E. coli*, *P. aeruginosa*, *S. aureus*, and *S. pyogenus*, respectively. Additionally, the MIC was found to be 100, 125, and 100 µg/mL for the antifungal species *C. albicans*, *A. niger*, and *A. clavatus*, respectively. These findings were compared with standard antimicrobial drugs available in the market.

In our study, the antimicrobial activity of AZOME extract was consistent with previous findings by Yousfi et al. (2021), who reported MIC values for *S. aureus* (1.44 mg/mL) and *P. aeruginosa* (0.72 mg/mL). We conducted a comprehensive assessment of secondary metabolites in the AZOME extract using qualitative and quantitative experimental assays. Qualitative phytochemical screening confirmed the presence of Saponins, Phenols, Alkaloids, Amino acids, Molish (carbohydrate) detection, and reducing sugars, while terpenoids were absent, consistent with findings by Osabor et al. (2015).

The Quantitative analysis provided further insights into secondary metabolites, with total phenolic content (TPC), total flavonoid content (TFC), and total flavonol content measured at 27.9±0.27 mg/g GAE, 18.4 mg/g QE, and 41.4±4 mg/g QE, respectively. These results enhance our understanding of the phytochemical composition of the AZOME extract.

The secondary metabolites found in the AZOME extract boast a rich polyphenol content, renowned for their potent antioxidant properties. These compounds act as guardians in the biological system, warding off diseases triggered by the presence of reactive oxygen species (ROS). Imagine them as vigilant sentinels, tirelessly neutralizing harmful radicals to maintain cellular harmony and health.

Assessment of the AZOME extract's antioxidant prowess was meticulously conducted through various *in vitro* assays. In the

DPPH assay, akin to a colorful chemistry experiment, the extract and standard ascorbic acid exhibited antioxidant activity by transforming the deep purple DPPH radical into a pale-yellow hue, indicating their efficacy in scavenging free radicals. The AZOME extract displayed an IC_{50} value of 353 µg/mL, showcasing its antioxidant potency.

Furthermore, the extract's ability to reduce Fe^3+ to Fe^2+ was assessed through the reducing power assay (RPA) and the Ferric Reducing Antioxidant Power (FRAP) assay. Like skilled alchemists, the extract demonstrated its capacity to donate hydrogen atoms or electrons to reactive species, thus mitigating ROS generation.

In the hydrogen peroxide assay, reminiscent of a battle against oxidative stress, the AZOME extract exhibited remarkable scavenging ability against H_2O_2 generation, with an IC_{50} value of 600 µg/mL. Additionally, the ABTS assay provided further evidence of the extract's antioxidant prowess. As the concentration of the AZOME extract increased, its electron donation to ABTS+ resulted in a fading of its color, indicative of antioxidant activity (Offei-Oknye et al. 2015; Hosseini et al. 2024).

The WHO Global Report paints a concerning picture of diabetes prevalence, with cases soaring from 135 million in 1995 to a staggering 300 million in 2025, and projected to reach 783 million by 2045. This epidemic is particularly pronounced in emerging nations like China, the US, and India, where the burden of diabetes is expected to be high (Kumar et al., 2024). Amidst this alarming trend, targeting key enzymes like alpha-amylase and alpha-glucosidase emerges as a crucial strategy in managing diabetic conditions.

These enzymes were pivotal players in carbohydrate metabolism, catalyzing the breakdown of complex carbohydrates into glucose monosaccharides, thus contributing to postprandial hyperglycemia. Inhibition of these enzymes can help regulate blood glucose levels. The AZOME extract exhibited significant inhibitory activity against alpha-amylase and alpha-glucosidase, with IC_{50} values of 1564.43 µg/mL and 581.4 µg/mL, respectively, comparable to positive controls like metformin and acarbose (Kumar et al., 2024). Similar findings were reported by Adeyeoluwa et al. (2020), highlighting the effectiveness of ginger extract in enzyme inhibition assays.

Furthermore, *in vitro* studies on L6 cell lines, mimicking skeletal muscle glucose uptake, revealed the AZOME extract's potential in enhancing glucose transport. At concentrations ranging from 133.32 to 533.3 µg/mL, the extract demonstrated a dose-dependent increase in glucose uptake, reaching 254.74±62.79 µg/mL at 533.3 µg/mL. This effect was comparable to the positive control metformin and insulin, indicating the extract's ability to stimulate glucose uptake in muscle cells (Kumar et al., 2024). Additionally, the extract's impact on GLUT1 expression and activation of AMPK and PI3-Kinase pathways further elucidates its mechanism of action in improving glucose absorption (Noipha and Ninla-Aesong, 2018).

The hyperglycemic state in individuals with diabetes leads to the formation of advanced glycation end products (AGEs), which contribute to secondary complications (Mohd Dom et al., 2020). Addressing this, there's a growing interest in natural inhibitors as alternatives to synthetic drugs. *In vitro* studies utilizing the BSA-AGE model demonstrated the significant antiglycation activity of AZOME extract, reducing AGEs formation by 58.59%, compared to the positive control (BSA+D-R), which showed 100% AGEs formation. This effect was comparable to the standard drug aminoguanidine, which reduced AGEs formation by 51.99% (Mohd Dom et al., 2020).

Congo-red (CR) dye was employed to detect amyloid formation in protein structures resulting from non-enzymatic reactions, leading to protein aggregation and fibrillation. AZOME extract showed promising results, reducing protein aggregation from 87.32% to 51.26%, similar to the effect of aminoguanidine, which decreased absorbance from 79.57% to 26.33% (Mohd Dom et al., 2020).

UV-Vis spectrum analysis provided further insights into the D-ribose-induced glycation model, highlighting enhanced hyperchromicity due to alterations in protein structure and glycation adduct formation. Treatment with aminoguanidine and AZOME extract (2.5-100 µg/mL) reduced hyperchromicity, suggesting hindrance in D-ribose attachment to protein-free amino acids, impeding glycated adduct formation (Nabi et al., 2018).

By the end of the study (7th day), both aminoguanidine and AZOME extract demonstrated decreased levels of glycated products, from 4.14% to 2.09% and from 7.5% to 3.47%, respectively, indicating the potential of AZOME extract in mitigating glycation-associated complications (Mohd Dom et al., 2020).

For the biosafety evaluation of AZOME extract, hemolysis assay and *in vitro* cytotoxicity assessment on healthy RAW 264.7 cells were conducted (Abdullah et al., 2023). Hemolysis activity of AZOME extract ranged from -0.399±0.020% to -0.305±0.031% at concentrations of 40-120 µg/mL, indicating negligible hemolytic activity, classified as non-hemolytic according to ASTM (American Society for Materials and Testing) standards (Abdullah et al., 2023). *In vitro* cell culture studies on RAW 264.7 cells revealed AZOME extract doses (25-1000 µg/mL) to be safe and non-toxic, with a proliferation rate reaching 99%. This aligns with findings by Zheng et al., where ginger polysaccharide exhibited a proliferation rate of 132.1% on RAW 264.7 cells (Zheng et al., 2024).

To identify lead compounds responsible for the antidiabetic property, GC-MS analysis of AZOME extract revealed 36 phytocompounds, subsequently docked with targeted proteins, including α-amylase (1b2y), α-glucosidase (3top), and GLUT4 (7wsm) (Mandal et al., 2018). Molecular docking simulations using

CB-DOCK2, PyRx, and Auto Dock Tools showed AZOME-derived phytocompounds exhibiting higher binding energy (docking score), indicating favorable interactions with the active binding sites of targeted proteins, similar to standard drugs like Metformin, Acarbose, and 2-DGP (Mandal et al., 2018).

The docking results of protein-ligand complexes, including binding affinity in kcal/mol and inhibition constant (mM/μM/nM) values, were determined, while the 3D and 2D confirmations, along with protein-ligand interactions and spacing of the grid box (Å), were outlined. Notably, various phytocompounds (ligands) such as Curcumin, Zingiberene, Beta-Bisabolene, Zingiberenol, β-eudesmol, Carotol, Caryophyllene oxide, Aromadendrene oxide, and Gamma-Sitosterol demonstrated significant binding affinities (in kcal/mol) with targeted antidiabetic proteins (1b2y, 3top, and 7wsm) (Mandal et al., 2018).

Similarly, standard drugs like metformin, acarbose, and 2-DGP were also docked with the targeted proteins and analyzed using Auto Dock Tools software and CB-DOCK2 and PyRx software. Results showed high docking scores, indicating favorable interactions with the active binding sites of the proteins (Mandal et al., 2018).

The comprehensive investigation revealed that AZOME extract contains abundant bioactive compounds with diverse therapeutic potentials, including antioxidant, antimicrobial, antidiabetic, and antiglycation properties.

Conclusion

In conclusion, the findings from our study suggest that AZOME extract holds promise for extensive applications in medicine, cosmetics, and food industries. Our experimental results underscore its potential as a rich source of phenolics and antioxidant phytocompounds, which exhibit robust free radical scavenging activity across various *in vitro* antioxidant assays. Moreover, AZOME demonstrates potent antimicrobial properties against both Gram-positive and Gram-negative microbial strains.

Of particular significance is its potential as a prophylactic and therapeutic agent for diabetic patients. Our study revealed compelling results in *in vitro* enzyme inhibition assays and glucose uptake studies using L6 cell lines, indicating promising antidiabetic properties. Additionally, AZOME showed efficacy in mitigating the formation of glycation adducts, addressing secondary complications in diabetic patients.

The *in silico* approach further supports these findings, revealing a strong binding affinity towards targeted antidiabetic proteins. Importantly, our investigation found no cytotoxic effects of AZOME extract, ensuring its safety for use.

Looking ahead, future research should include *in vivo* studies to validate the *in vitro* and *in silico* antidiabetic findings, thereby providing a more comprehensive understanding of AZOME's therapeutic potential. Overall, these findings highlight AZOME extract as a promising candidate for the development of novel therapeutics targeting various health conditions.

Author contributions

M.H.M., and T.K.U. have designed the experiments. M.H.M., T.K.U., and P.S.M. have performed phytochemical extraction. M.H.M. and T.K.U. have done the experimental work. M.H.M. and T.K.U. drafted the manuscript. M.H.M., V.J.U., and T.K.U. collected relevant literature information. All authors have read and approved the final manuscript.

Acknowledgment

The authors expressed their deep gratitude to Dr. Geetika Madan Patel, Medical Director and Vice President of the Research and Development Cell (RDC) at Parul University, for providing a sophisticated research facility and financial support through an Intramural Research Project (CR4D/IMSL/047). They also thanked the RDC team and the lab members of Animal Cell Culture and Immunobiochemistry, Lab-105. Additionally, they were grateful to the Director of RDC for access to the Central Research Facility and to the Government of Gujarat for fellowship support under the SHODH Scheme. Special thanks to Dr. Tarun K. Upadhyay for his constant guidance and support throughout this research.

Competing financial interests

The authors have no conflict of interest.

References

Abdullah, Hussain T, Faisal S, Rizwan M, Almostafa MM, Younis NS, Yahya G (2023) Zingiber officinale rhizome extracts mediated ni nanoparticles and its promising biomedical and environmental applications. BMC Complementary Medicine and Therapies 23 (1):349. https://doi.org/10.1186/s12906-023-04182-7

Adeyeoluwa TE, Balogun FO, Ashafa AOT (2020) In vitro comparative assessment of the inhibitory effects of single and combined spices against glucose-synthesizing enzymes. Tropical Journal of Pharmaceutical Research 19 (6):1209-1214. https://doi.org/10.4314/tjpr.v19i6.14

Akbari S, Abdurahman NH, Yunus RM, Alara OR, Abayomi OO (2019) Extraction, characterization and antioxidant activity of fenugreek (Trigonella-Foenum Graecum) seed oil. Materials Science for Energy Technologies 2 (2):349-355. https://doi.org/10.1016/j.mset.2018.12.001

Ali A, Gilani AH (2007) Medicinal value of ginger with focus on its use in nausea and vomiting of pregnancy. International Journal of Food Properties 10 (2):269-278. https://doi.org/10.1080/10942910601045297

Ali BH, Blunden G, Tanira MO, Nemmar A (2008) Some phytochemical, pharmacological and toxicological properties of ginger (Zingiber officinale Roscoe): a review of recent research. Food and chemical Toxicology 46 (2):409-420.https://doi.org/10.1016/j.fct.2007.09.085

Al-Mustafa A, Al-Tawarah M, Al-Sheraideh MS, Al-Zahrany FA (2021) Phytochemical analysis, antioxidant and in vitro β-galactosidase inhibition activities of Juniperus

phoenicea and Calicotome villosa methanolic extracts. BMC chemistry 15:1-13. https://doi.org/10.1186/s13065-021-00781-y

Alsahli MA, Almatroodi SA, Almatroudi A, Khan AA, Anwar S, Almutary AG, Alrumaihi F, Rahmani AH (2021) 6-Gingerol, a major ingredient of ginger attenuates diethylnitrosamine-induced liver injury in rats through the modulation of oxidative stress and anti-inflammatory activity. Mediators of inflammation 2021:1-17. https://doi.org/10.1155/2021/6661937 33

Alvi SS, Nabi R, Khan M, Akhter F, Ahmad S, Khan MS (2021) Glycyrrhizic acid scavenges reactive carbonyl species and attenuates glycation-induced multiple protein modification: an in vitro and in silico study. Oxidative Medicine and Cellular Longevity 2021. https://doi.org/10.1155/2021/7086951

Ashraf JM, Rabbani G, Ahmad S, Hasan Q, Khan RH, Alam K, Choi I (2015) Glycation of H1 histone by 3-deoxyglucosone: effects on protein structure and generation of different advanced glycation end products. PLoS One 10 (6):e0130630. https://doi.org/10.1371/journal.pone.0130630

Bahuguna A, Khan I, Bajpai VK, Kang SC (2017) MTT assay to evaluate the cytotoxic potential of a drug. ||| Bangladesh Journal of Pharmacology 12 (2):115-118. https://doi.org/10.3329/bjp.v12i2.30892

Banday MZ, Sameer AS, Nissar S (2020) Pathophysiology of diabetes: An overview. Avicenna journal of medicine 10 (04):174-188. https://doi.org/10.4103/ajm.ajm_53_20

Beristain-Bauza SDC, Hernández-Carranza P, Cid-Pérez TS, Ávila-Sosa R, Ruiz-López II, Ochoa-Velasco CE (2019) Antimicrobial activity of ginger (Zingiber officinale) and its application in food products. Food Reviews International 35 (5):407-426. https://doi.org/10.1080/87559129.2019.1573829

Eid BG, Mosli H, Hasan A, El-Bassossy HM (2017) Ginger ingredients alleviate diabetic prostatic complications: Effect on oxidative stress and fibrosis. Evidence-based complementary and alternative medicine 2017. https://doi.org/10.1155/2017/6090269

Fernandes RdPP, Trindade MA, Tonin FG, Lima CGd, Pugine SMP, Munekata PES, Lorenzo J, De Melo M (2016) Evaluation of antioxidant capacity of 13 plant extracts by three different methods: cluster analyses applied for selection of the natural extracts with higher antioxidant capacity to replace synthetic antioxidant in lamb burgers. Journal of food science and technology 53:451-460. https://doi.org/10.1007/s13197-015-1994-x

Gohel A, Upadhye V, K Upadhyay T, Rami E, Panchal R, Jadhav S, Dhakane R, Kele V (2021) Study on phytochemical screening and antimicrobial activity of Adhatoda vasica. Canadian Journal of Medicine 3 (3):105-113. https://doi.org/10.33844/cjm.2021.60509

Hafeez J, Naeem M, Ali T, Sultan B, Hussain F, Ur Rashid H, Nadeem M, Shirzad I (2023) Comparative Study of Antioxidant, Antidiabetic, Cytotoxic Potentials, and Phytochemicals of Fenugreek (Trigonella foenum-graecum) and Ginger (Zingiber officinale). Journal of Chemistry 2023. https://doi.org/10.1155/2023/3469727

Hasan Mujahid M, Upadhyay TK, Upadhye V, Sharangi AB, Saeed M (2023) Phytocompound identification of aqueous Zingiber officinale rhizome (ZOME) extract reveals antiproliferative and reactive oxygen species mediated apoptotic induction within cervical cancer cells: an in vitro and in silico approach. Journal of Biomolecular Structure and Dynamics:1-28. https://doi.org/10.1080/07391102.2023.2247089

Hassan LEA, Al-Suede FS, Fadul SM, Abdul Majid AMS. (2018). Evaluation of antioxidant, antiangiogenic and antitumor properties of Anogeissus leiocarpus against colon cancer. Angiotherapy, 1(2), pages 056–066.

Hosseini A, Alavi MS, Toos MGN, Jamialahmadi T, Sahebkar A (2024) 6-Gingerol, an ingredient of Zingiber officinale, abrogates lipopolysaccharide-induced cardiomyocyte injury by reducing oxidative stress and inflammation. Journal of Agriculture and Food Research 15:101034. https://doi.org/10.1016/j.jafr.2024.101034

Husen A (2023) Antidiabetic medicinal plants and herbal treatments. CRC Press. https://doi.org/10.1201/b23347

Huyut Z, Beydemir Ş, Gülçin İ (2017) Antioxidant and antiradical properties of selected flavonoids and phenolic compounds. Biochemistry research international 2017. https://doi.org/10.1155/2017/7616791

Iza Safany Che Hanafi, Chandrarohini Saravanan, Rabiatul Basria S. M. N. Mydin. (2024). Oxidative Stress: Insights into Nutrition, Psychological Stress, Environmental Exposure, and Antioxidants Roles, Journal of Angiotherapy, 8(3), 1-5, 9452

Javed Ahamad. (2023a). Characterization of Essential Oil Composition of Syzygium aromaticum Linn. (Clove) by GC-MS and Evaluation of its Antioxidant Activity, Journal of Angiotherapy, 7(1), 1-5

Jiang C, Wang L, Shao J, Jing H, Ye X, Jiang C, Wang H, Ma C (2020) Screening and identifying of α-amylase inhibitors from medicine food homology plants: Insights from computational analysis and experimental studies. Journal of Food Biochemistry 44 (12):e13536. https://doi.org/10.1111/jfbc.13536

Jung H, Kim YS, Jung D-M, Lee K-S, Lee J-M, Kim KK (2022) Melittin-derived peptides exhibit variations in cytotoxicity and antioxidant, anti-inflammatory and allergenic activities. Animal Cells and Systems 26 (4):158-165. https://doi.org/10.1080/19768354.2022.2099971

Khan F, Pandey P, Singh A, Upadhyay TK, AboElnaga SMH, Al-Najjar MA, Saeed M, Kahrizi D (2022) Unveiling Antioxidant and Antiproliferative Effects of Prosopis juliflora Leaves against Human Prostate Cancer LNCaP Cells. Cellular and Molecular Biology 68 (11):20-27. https://doi.org/10.14715/cmb/2022.68.11.4

Kumar A, Gangwar R, Ahmad Zargar A, Kumar R, Sharma A (2024) Prevalence of diabetes in India: A review of IDF diabetes atlas 10th edition. Current diabetes reviews 20 (1):105-114. https://doi.org/10.2174/1573399819666230413094200

Kurhekar JV (2021) Ancient and modern practices in phytomedicine. In: Preparation of Phytopharmaceuticals for the Management of Disorders. Elsevier, pp 55-75. https://doi.org/10.1016/b978-0-12-820284-5.00019-8

Kusse Gudishe Goroya KGG, Zewde Mitiku ZM, Yoseph Alresawum Asresahegn YAA (2019) Determination of concentration of heavy metals in ginger using flame atomic absorption spectroscopy.https://doi.org/10.5897/ajps2019.1787

Liu Y, Yang X, Gan J, Chen S, Xiao Z-X, Cao Y (2022) CB-Dock2: Improved protein–ligand blind docking by integrating cavity detection, docking and homologous template fitting. Nucleic acids research 50 (W1):W159-W164. https://doi.org/10.1093/nar/gkac394

Ma R-H, Ni Z-J, Zhu Y-Y, Thakur K, Zhang F, Zhang Y-Y, Hu F, Zhang J-G, Wei Z-J (2021) A recent update on the multifaceted health benefits associated with ginger and its bioactive components. Food & Function 12 (2):519-542. https://doi.org/10.1039/d0fo02834g

Mandal SP, Garg A, Prabitha P, Wadhwani AD, Adhikary L, Kumar BP (2018) Novel glitazones as PPARγ agonists: molecular design, synthesis, glucose uptake activity and 3D QSAR studies. Chemistry Central Journal 12:1-21. https://doi.org/10.1186/s13065-018-0508-0

Mohammadinejad R, Shavandi A, Raie DS, Sangeetha J, Soleimani M, Hajibehzad SS, Thangadurai D, Hospet R, Popoola JO, Arzani A (2019) Plant molecular farming: production of metallic nanoparticles and therapeutic proteins using green factories. Green chemistry 21 (8):1845-1865. https://doi.org/10.1039/c9gc00335e

Mohd Dom NS, Yahaya N, Adam Z, Hamid M (2020) Antiglycation and antioxidant properties of Ficus deltoidea varieties. Evidence-Based Complementary and Alternative Medicine 2020. https://doi.org/10.1155/2020/6374632

Mostafa Alamholo. (2024). Determination of Active Biomarkers and the Antioxidant and Antibacterial Potential of Standardized Zygophyllum spp Extract. Journal of Angiotherapy, 8(1), 1-10, 9369

Nabi R, Alvi SS, Khan RH, Ahmad S, Ahmad S, Khan MS (2018) Antiglycation study of HMG-R inhibitors and tocotrienol against glycated BSA and LDL: A comparative study. International journal of biological macromolecules 116:983-992. https://doi.org/10.1016/j.ijbiomac.2018.05.115

Nabi R, Alvi SS, Saeed M, Ahmad S, Khan MS (2019) Glycation and HMG-CoA reductase inhibitors: implication in diabetes and associated complications. Current diabetes reviews 15 (3):213-223. https://doi.org/10.2174/1573399814666180924113442

Nabi R, Alvi SS, Shah MS, Ahmad S, Faisal M, Alatar AA, Khan MS (2020) A biochemical & biophysical study on in-vitro anti-glycating potential of iridin against D-Ribose modified BSA. Archives of biochemistry and biophysics 686:108373. https://doi.org/10.1016/j.abb.2020.108373

Nariya PB, Bhalodia NR, Shukla V, Acharya R (2011) Antimicrobial and antifungal activities of Cordia dichotoma (Forster F.) bark extracts. AYU (An international quarterly journal of research in Ayurveda) 32 (4):585-589. https://doi.org/10.4103/0974-8520.96138

Nguyen ST, Vo PH, Nguyen TD, Do NM, Le BH, Dinh DT, Truong KD, Van Pham P (2019) Ethanol extract of Ginger Zingiber officinale Roscoe by Soxhlet method induces apoptosis in human hepatocellular carcinoma cell line. Biomedical Research and Therapy 6 (11):3433-3442. https://doi.org/10.15419/bmrat.v6i11.572

Noipha K, Ninla-Aesong P (2018) Antidiabetic activity of Zingiber officinale Roscoe rhizome extract: an in vitro study. HAYATI Journal of Biosciences 25 (4):160-160. https://doi.org/10.4308/hjb.25.4.160

Nur Royhaila Mohamad, Farrah Payyadhah Borhan, Mohd Shahrizi Razali, Roswanira Abdul Wahab, (2023), Optimizing The Protocol For Extraction Of Bioactive Components From Hibiscus Sabdariffa With Potent Antioxidant Activity, Journal of Angiotherapy, 7(1), 1-9

Nurr Maria Ulfa Seruji, Vivien Jong Yi Mian, Nor Hisam Zamakshari et al., (2023), Antioxidant Potential of Calophyllum gracilentum: A Study on Total Phenolic Content, Total Flavonoid Content, and Free Radical Scavenging Activities, Journal of Angiotherapy, 7(1), 1-8

Offei-Oknye R, Patterson J, Walker L, Verghese M (2015) Processing effects on phytochemical content and antioxidative potential of ginger Zingiber officale. Food and Nutrition Sciences 6 (5):445-451. https://doi.org/10.4236/fns.2015.65046

Osabor V, Bassey F, Umoh U (2015) Phytochemical screening and quantitative evaluation of nutritional values of Zingiber officinale (Ginger). American Chemical Science Journal 8 (4):1-6. https://doi.org/10.9734/acsj/2015/16915

Oyedemi S, Bradley G, Afolayan A (2012) In vitro and in vivo antioxidant properties of aqueous extract from Strychnos henningsii Gilg stem bark. Free Radical Biology and Medicine (53):S113. https://doi.org/10.1016/j.freeradbiomed.2012.08.237

Oyedemi SO, Oyedemi BO, Ijeh II, Ohanyerem PE, Coopoosamy RM, Aiyegoro OA (2017) Alpha-amylase inhibition and antioxidative capacity of some antidiabetic plants used by the traditional healers in Southeastern Nigeria. The Scientific World Journal 2017. https://doi.org/10.1155/2017/3592491

Papoutsis K, Zhang J, Bowyer MC, Brunton N, Gibney ER, Lyng J (2021) Fruit, vegetables, and mushrooms for the preparation of extracts with α-amylase and α-glucosidase inhibition properties: A review. Food Chemistry 338:128119. https://doi.org/10.1016/j.foodchem.2020.128119

Rhee SY, Kim YS (2018) The role of advanced glycation end products in diabetic vascular complications. Diabetes & metabolism journal 42 (3):188. https://doi.org/10.4093/dmj.2017.0105

Richards C, O'Connor N, Jose D, Barrett A, Regan F (2020) Selection and optimization of protein and carbohydrate assays for the characterization of marine biofouling. Analytical methods 12 (17):2228-2236. https://doi.org/10.1039/d0ay00272k

Sahoo MR, Umashankara MS (2023) FTIR Based metabolomics profiling and fingerprinting of some medicinal plants: an attempt to develop an approach for quality control and standardization of herbal materials. Pharmacognosy Research 15 (1). https://doi.org/10.5530/097484900288

Salehi B, Martorell M, Arbiser JL, Sureda A, Martins N, Maurya PK, Sharifi-Rad M, Kumar P, Sharifi-Rad J (2018) Antioxidants: positive or negative actors? Biomolecules 8 (4):124. https://doi.org/10.3390/biom8040124

Saraf S (2012) Development of Fingerprinting Methods of Balacaturbhadrika Churna: An Ayurvedic Formulation. Pharmacognosy Journal 4 (27):20-24. https://doi.org/10.5530/pj.2012.27.3

Shah A, Niaz A, Ullah N, Rehman A, Akhlaq M, Zakir M, Suleman Khan M (2013) Comparative study of heavy metals in soil and selected medicinal plants. Journal of Chemistry 2013. https://doi.org/10.1155/2013/621265

Sivasothy Y, Chong WK, Hamid A, Eldeen IM, Sulaiman SF, Awang K (2011) Essential oils of Zingiber officinale var. rubrum Theilade and their antibacterial activities. Food chemistry 124 (2):514-517. https://doi.org/10.1016/j.foodchem.2010.06.062

Slowing II, Wu CW, Vivero-Escoto JL, Lin VSY (2009) Mesoporous silica nanoparticles for reducing hemolytic activity towards mammalian red blood cells. Small 5 (1):57-62. https://doi.org/10.1002/smll.200800926

Srinivasan K (2017) Ginger rhizomes (Zingiber officinale): A spice with multiple health beneficial potentials. PharmaNutrition 5 (1):18-28. https://doi.org/10.1016/j.phanu.2017.01.001

Telagari M, Hullatti K (2015) In-vitro α-amylase and α-glucosidase inhibitory activity of Adiantum caudatum Linn. and Celosia argentea Linn. extracts and fractions. Indian journal of pharmacology 47 (4):425-429. https://doi.org/10.4103/0253-7613.161270

Trott O, Olson AJ (2010) AutoDock Vina: improving the speed and accuracy of docking with a new scoring function, efficient optimization, and multithreading. Journal of computational chemistry 31 (2):455-461. https://doi.org/10.1002/jcc.21334

Twereen AK, Panezai MA, Sajjad A, Achakzai JK, Kakar AM, Khan NY (2021) Comparative analysis of antioxidant activity, toxicity, and mineral composition of kernel and pomace of apricot (Prunus armeniaca L.) grown in Balochistan, Pakistan. Saudi Journal of Biological Sciences 28 (5):2830-2839. https://doi.org/10.1016/j.sjbs.2021.02.015

Upadhyay TK, Das S, Mathur M, Alam M, Bhardwaj R, Joshi N, Sharangi AB (2024) Medicinal plants and their bioactive components with antidiabetic potentials. Antidiabetic Medicinal Plants:327-364. https://doi.org/10.1016/b978-0-323-95719-9.00017-3

Vajrabhaya L-O, Korsuwannawong S (2016) Cytotoxicity evaluation of Clinacanthus nutans through dimethylthiazol diphenyltetrazolium bromide and neutral red uptake assays. European journal of dentistry 10 (01):134-138. https://doi.org/10.4103/1305-7456.175701

Valdés-Tresanco MS, Valdés-Tresanco ME, Valiente PA, Moreno E (2020) AMDock: a versatile graphical tool for assisting molecular docking with Autodock Vina and Autodock4. Biology direct 15:1-12. https://doi.org/10.1186/s13062-020-00267-2

Vishwanath D, Srinivasan H, Patil MS, Seetarama S, Agrawal SK, Dixit M, Dhar K (2013) Novel method to differentiate 3T3 L1 cells in vitro to produce highly sensitive adipocytes for a GLUT4 mediated glucose uptake using fluorescent glucose analog. Journal of cell communication and signaling 7 (2):129-140. https://doi.org/10.1007/s12079-012-0188-9

Visvanathan R, Jayathilake C, Liyanage R (2016) A simple microplate-based method for the determination of α-amylase activity using the glucose assay kit (GOD method). Food chemistry 211:853-859. https://doi.org/10.1016/j.foodchem.2016.05.090

Warren FJ, Zhang B, Waltzer G, Gidley MJ, Dhital S (2015) The interplay of α-amylase and amyloglucosidase activities on the digestion of starch in in vitro enzymic systems. Carbohydrate polymers 117:192-200. https://doi.org/10.1016/j.carbpol.2014.09.043

Yousfi F, Abrigach F, Petrovic J, Sokovic M, Ramdani M (2021) Phytochemical screening and evaluation of the antioxidant and antibacterial potential of Zingiber officinale extracts. South African Journal of Botany 142:433-440. https://doi.org/10.1016/j.sajb.2021.07.010

Zheng Q, Cheng Z, Duan Y, Hu K, Cai M, Zhang H (2024) Effect of subcritical water temperature on the chain conformation and immune activity of ginger polysaccharides. International Journal of Biological Macromolecules 261:129833. https://doi.org/10.1016/j.ijbiomac.2024.129833